Hyperperfusion of Frontal White and Subcortical Gray Matter in Autism Spectrum Disorder

Supplemental Information
Table of Contents

SECTION 7: PRIMARY ANALYSES SEPARATELY IN YOUTH AND ADULTS

SUPPLEMENTAL TEXT

Section 1: MRI Scanning Procedures and Pulse Sequences

Images were acquired on a GE Signa 3T (Tesla) HDx system with an 8-channel, receive-only head coil.

ASL We optimized our Pulsed Arterial Spin Labeling (PASL) perfusion sequence for parallel imaging at 3T using a PICORE (Proximal Inversion with Control for Off-Resonance Effects) QUIPSS II (Quantitative Imaging of Perfusion using a Single Subtraction) pulse sequence (1). We placed a 9-cm tagging slab 16-mm below the proximal edge of the imaging volume. We acquired the control images by applying off-resonance adiabatic hyperbolic secant RF pulse with the same frequency offset as that for the labeled images without the slice-selective gradient, so as to control for off-resonance effects of the inversion pulses used for acquiring the labeled images. We used a single-shot, gradient-echo, echo planar imaging (EPI) sequence for image acquisition, with time to QUIPSS saturation TI_1=600 ms and inversion time of the first slice TI_2 =1300 ms. Acquisition parameters included FOV 24 cm, 64x64 matrix, TE(echo time)/TR (repetition time)=24/2300ms, flip angle 90°, slice thickness 6 mm, inter-slice spacing 0.5 mm, providing a nominal spatial resolution of 3.75x3.75x6.5 mm. We acquired 18 slices from inferior to superior in sequential order. Each ASL scan with 151 acquisitions plus 5 dummy images required 5 min 59 sec.

A separate M0 scan using gradient-echo EPI with TR of 15sec was acquired at the same resolution and slice position as the ASL data. The M_{0wm} from white matter is measured and then used in the off-line computation of rCBF (1).

ASL Localizer We also acquired a T1-weighted, localizer image with high in-plane resolution in the same slice locations as the ASL data for coregistering each participant's ASL data to its T1-weighted anatomical MR image. The localizer image was acquired using a 2D, fast spin echo pulse sequence with echo train length=9, TR = 2150ms, TE = 9.94ms, TI = 840ms, flip angle = 90^o, in-plane resolution = 0.94 x 0.94 mm^2, slice thickness = 6.5mm. Total acquisition time = 1 min, 46 sec.

MRS data were acquired in 6 axial-oblique slabs (2-mm gap) parallel to the anterior commissure-posterior commissure (AC-PC): one slab below, one slab containing, and 4 slabs above the AC-PC. We used a water-suppressed MPCSI sequence with TR/TE=2800/144 ms, voxels 10x10x10 mm^3, and suppressed lipid signal from the scalp using eight saturation bands. Scan time, including shimming, was 20 min.

MRS Localizer A "localizer" MRI with voxels 0.98x0.98x10 mm^3 was acquired in register with MPCSI and was used to coregister and normalize MPCSI data into the common coordinate space of a template brain. Whole-brain T1-weighted (T1) MRI was obtained using 3D spoiled gradient recall with 0.98x0.98x1.0 mm^3 voxels. The T1 was used to prescribe MPCSI and to segment the brain into gray and white matter.

Additional Sequences included Anatomical MRI, Diffusion Tensor Imaging, Task-Based functional MRI, and Resting-State functional MRI

Total Scan Time was approximately 75 minutes, with additional time included for participant breaks to rest and move about, and reacquire sequences that had evidence of motion artifact.

Section 2: Image Processing Methods

ASL We aligned the PASL brain images and the M_{0_WM} image to the first PASL image for each participant in native imaging space to correct for head motion. We spatially smoothed the coregistered PASL images using a Gaussian kernel of 6mm FWHM (Full Width at Half Maximum) to improve signal-to-noise ratio while avoiding loss of spatial precision in locating our effects of interest. We generated a brain mask for each participant based on the mean PASL image. We constructed for each participant a voxel-wise map of rCBF from the PASL time series and M_{0_WM} image using in-house software: (1) We pair-wise subtracted the control images from the labeled images; (2) From the average of the subtracted images, we calculated rCBF at each voxel as $rCBF = \frac{6000*\Delta I}{2\alpha*M_{0\_B}*TI_1*exp(-TI_2/T_{1\_B})}$, where ΔI is the image difference obtained in step 1; α is the tagging efficiency, for which we used the default value of 0.9; $TI_1 = 600$ ms is the time to QUIPSS saturation; $TI_2 = 1300$ ms is the inversion time of the first slice and is slice time corrected for the rest of the slices in the imaging volume; and T_{1B} is the T_1 of blood, for which we used the default value of 1664 ms (2); M_{0_B} is the MR signal from a voxel filled with arterial blood, estimated from the M_{0_WM} map as $M_{0\_B} = rM_{0\_WM}e^{(1/T_{2WM}-1/T_{2B})TE}$ where *r* is the proton density ratio of blood, for which we used a default value of 1.06; and where the default values for T_{2WM} and T_{2B} were 70 ms and 200 ms, respectively (1, 3, 4). We used a 6 degrees-of-freedom rigid-body transformation such that mutual information (5) is increased to coregister the anatomical images to the localizer images for each participant. Subsequently, each participant's anatomical image is used as an intermediary source to coregister the rCBF images to a template brain by applying a similarity (5) followed with a nonlinear transformation based on fluid flow (6). We selected a single individual brain as the template brain, which was morphologically the most representative of the brains for TD participants (7).

We quantified the amount of head motion in the ASL data of each participant using two summary statistics, Root Mean Squared (RMS) (8) and Mean Frame-wise Displacement (FD) metric sums differentiated realignment estimates (9), derived from three translational (x,y,z) and three angular rotational (roll, pitch, yaw). Motion during the ASL scan was minimal and comparable across groups (Table 1).

MRS Following time-domain preprocessing, MPCSI data were transformed into the frequency domain and loaded into a 3DiCSI software package (http://hatch.cpmc.columbia.edu/software.html) that identified brain-internal MPCSI voxels. Spectra were fit for NAA (N-acetylaspartate), Glx, Cr (creatine), Cho (choline) and lipids using Gaussian-Lorentzian curves and least-squares estimation. Areas under the curves estimated metabolite concentrations in each voxel. Data were quality controlled by inspection of each spectrum, rejecting spectra with lipid contamination, insufficient water suppression, unresolved Cr and Cho, or linewidth > 12 Hz. We calculated background noise as the standard deviation of the part of the real spectrum free from metabolite signal, then generated a spectroscopic image for NAA as the ratio of peak area to background noise for each voxel, accounting for variations in receiver and transmitter gain. The brain was extracted from each T1 volume, warped into a cross-participant template, and segmented into gray and white matter. We corrected the spectroscopic images for partial-voluming (variable gray- *vs.* white-matter content across MPCSI voxels) and for the MPCSI point-spread function (dispersion of the MR signal into neighboring voxels) using linear regression to estimate the concentration of that metabolite in gray matter and white matter in each voxel and neighboring voxels. We resampled metabolite levels from the low-resolution MPCSI to the high-resolution T1 during spatial normalization, which

required coregistering and nonlinearly warping the MPCSI volume for each participant onto the T1 template brain. We then used the T1 image and high-resolution localizer to coregister each metabolite image to the study template to permit correlation of NAA levels with rCBF measures at each voxel. Processing for the detection of lactate in this sample has been described in detail previously (10).

References

1. Wong EC, Buxton RB, Frank LR (1998): Quantitative imaging of perfusion using a single subtraction (QUIPSS and QUIPSS II). *Magn Reson Med*. 39:702-708.
2. Lu H, Clingman C, Golay X, van Zijl PC (2004): Determining the longitudinal relaxation time (T1) of blood at 3.0 Tesla. *Magn Reson Med*. 52:679-682.
3. Jarnum H, Steffensen EG, Knutsson L, Frund ET, Simonsen CW, Lundbye-Christensen S, et al. (2010): Perfusion MRI of brain tumours: a comparative study of pseudo-continuous arterial spin labelling and dynamic susceptibility contrast imaging. *Neuroradiology*. 52:307-317.
4. Alsop DC, Detre JA (1996): Reduced transit-time sensitivity in noninvasive magnetic resonance imaging of human cerebral blood flow. *J Cereb Blood Flow Metab*. 16:1236-1249.
5. Viola P, Wells, W. M. (1995): Alignment by Maximization of Mutual Information. *IEEE Proc of the 5th Int Conf on Computer Vision*. Boston, MA, pp 16-23.
6. Christensen GE, Joshi SC, Miller MI (1997): Volumetric Transformation of Brain Anatomy. *IEEE Transactions on Medical Imaging*. 16:1369-1383.
7. Peterson BS, Warner V, Bansal R, Zhu H, Hao X, Liu J, et al. (2009): Cortical thinning in persons at increased familial risk for major depression. *Proc Natl Acad Sci U S A*. 106:6273-6278.
8. Jenkinson M, Bannister P, Brady M, Smith S (2002): Improved optimization for the robust and accurate linear registration and motion correction of brain images. *Neuroimage*. 17:825-841.
9. Power JD, Barnes KA, Snyder AZ, Schlaggar BL, Petersen SE (2012): Spurious but systematic correlations in functional connectivity MRI networks arise from subject motion. *NeuroImage*. 59:2142-2154.
10. Goh S, Dong Z, Zhang Y, DiMauro S, Peterson BS (2014): Mitochondrial dysfunction as a neurobiological subtype of autism spectrum disorder: evidence from brain imaging. *JAMA psychiatry*. 71:665-671.

Supplemental Materials Section 3:
3a: Main Text Figures Showing All Slices

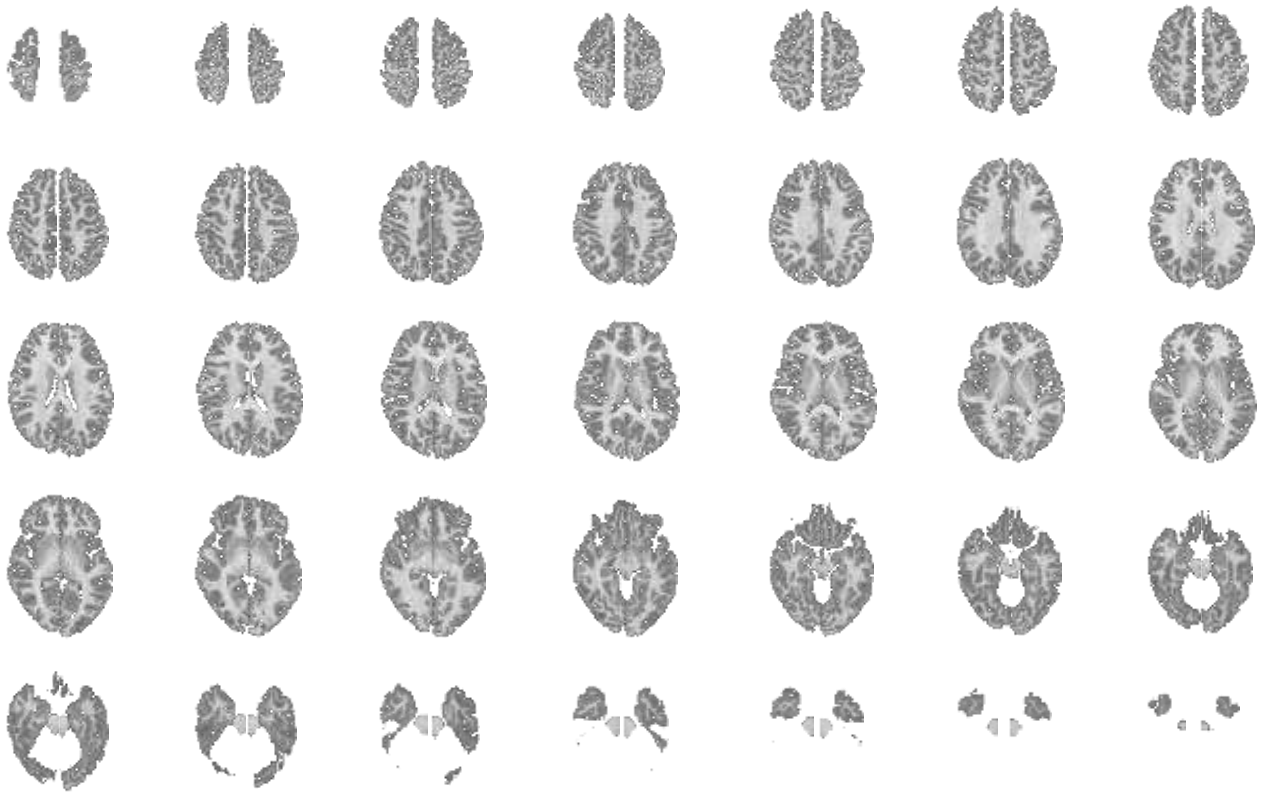

Supplementary Figure S1. T1-Weighted Anatomical Template
Shown are all slices of the T1-weighted anatomical template on which statistical maps were overlaid, with transaxial slice levels positioned parallel to the Anterior Commissure-Posterior Commissure (AC-PC) line. The z-values represent slice level (in millimeters) in the Talairach coordinate system. The right sides of the images correspond to the right side of the brain.

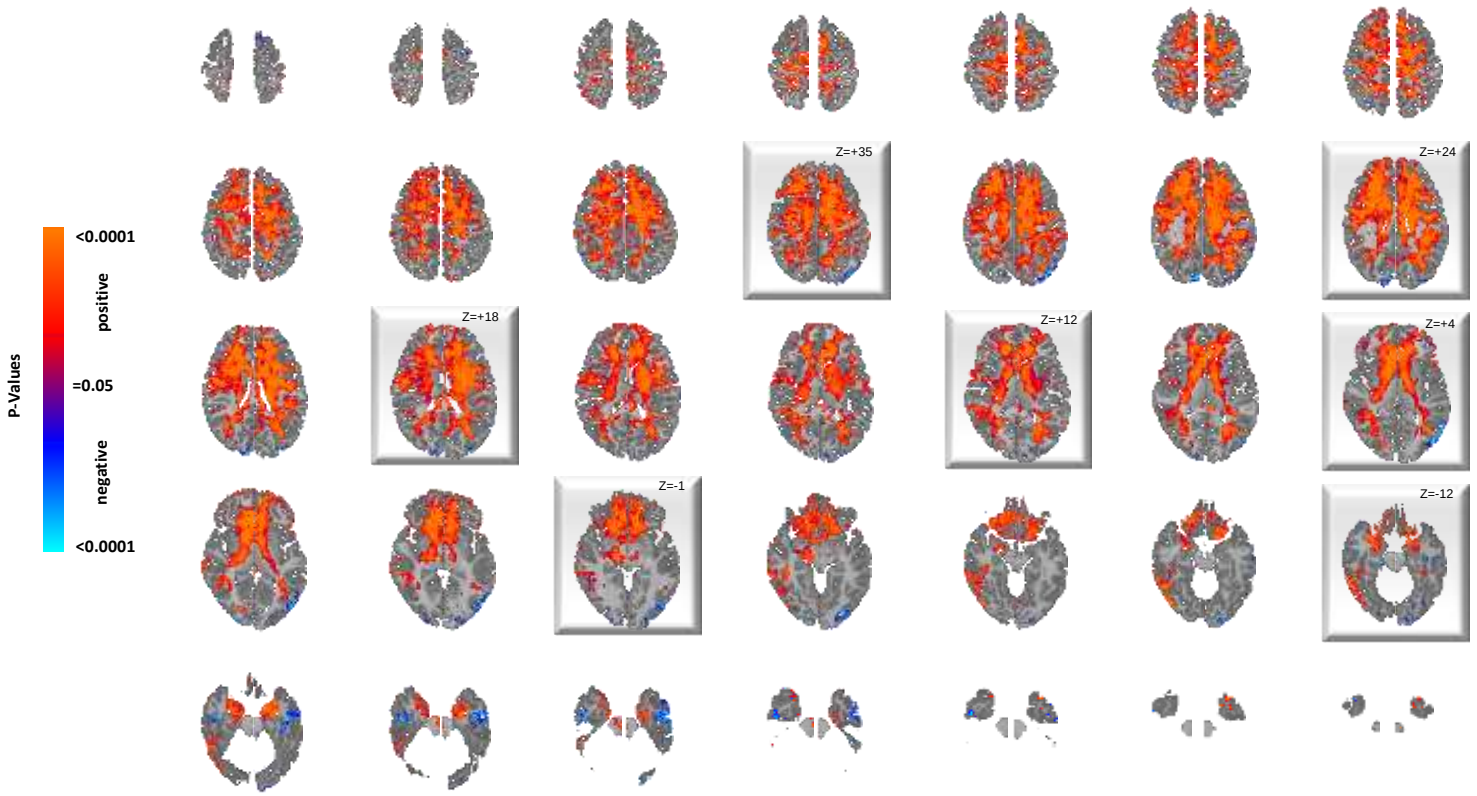

Supplementary Figure S2. Main Effect of Diagnosis for All Slices

This shows the statistically significant differences in rCBF values between the ASD group and TD controls for all slices while covarying for age and sex, displayed at a threshold of P<0.05 after correction for multiple comparisons. Voxels in red indicate significantly increased rCBF, and blue voxels reduced rCBF, in ASD relative to controls. Highlighted slices (with their z-level Talairach coordinates) are those displayed in Figure 1 of the main text.

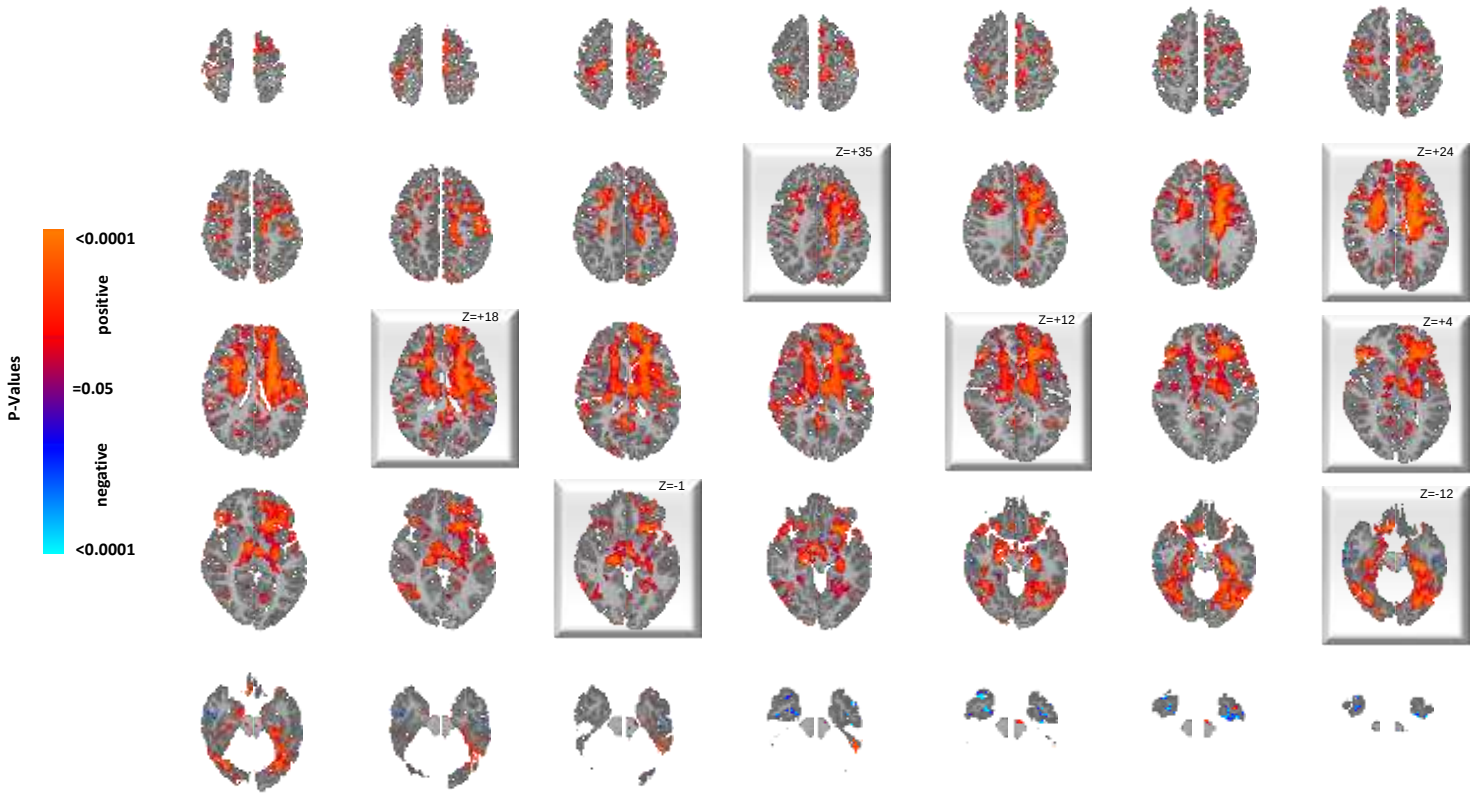

Supplementary Figure S3. Correlation of rCBF with ADOS Total Scores for All Slices

Shown here are all slices for the statistically significant correlations of ADOS Total scores with rCBF values in the ASD group, while covarying for age and sex, displayed at a threshold of P<0.05 after FDR correction for multiple comparisons. Red and blue voxels represent, respectively, significant positive or inverse correlations of ADOS Total scores with rCBF values in the ASD group. Highlighted slices (with their z-level Talairach coordinates) are those displayed in Figure 1 of the main text.

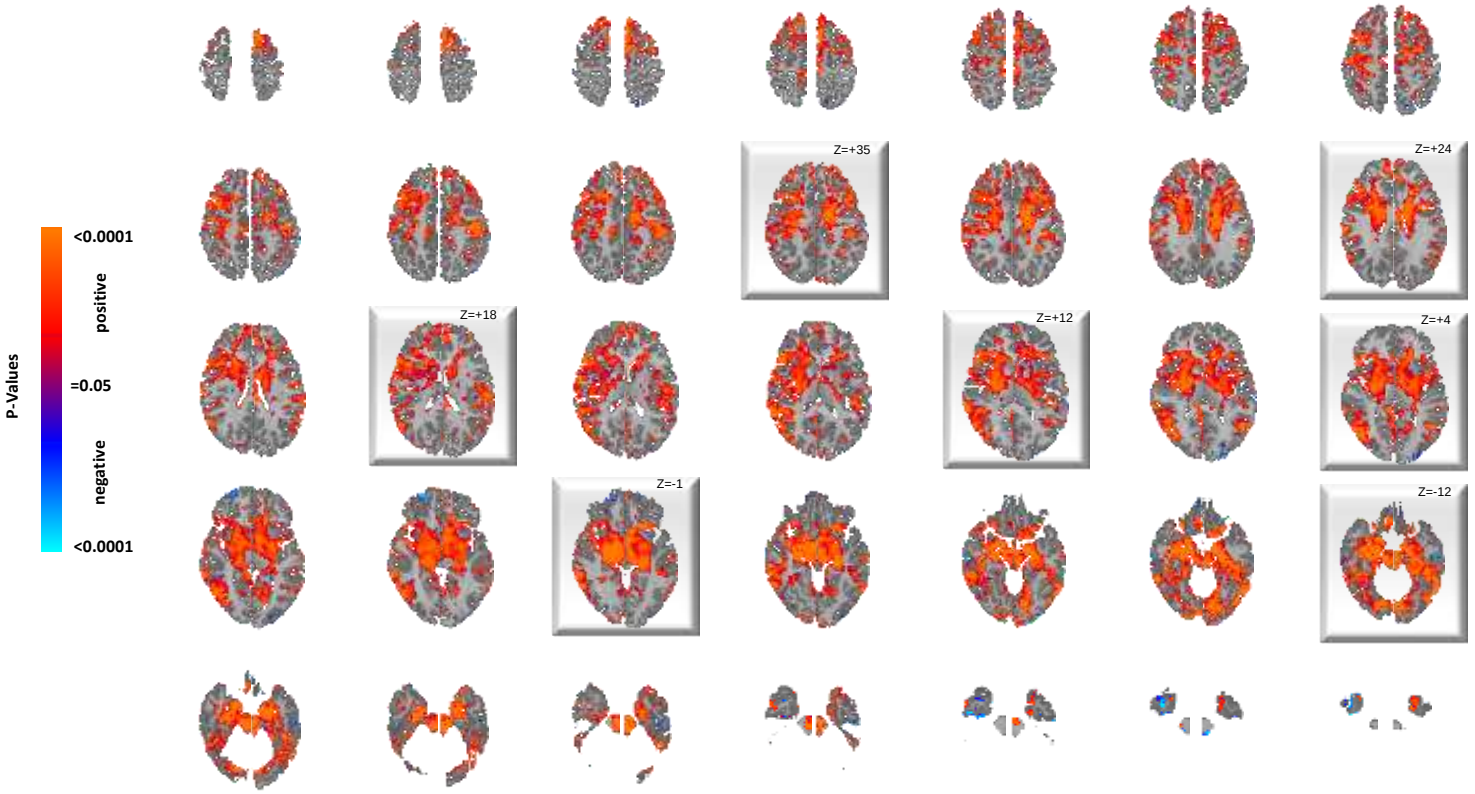

Supplementary Figure S4. Correlation of rCBF with SRS Social Awareness Scores for All Slices
Shown here are all slices for the statistically significant correlations of SRS Awareness scores with rCBF values in the ASD group, while covarying for age and sex, displayed at a threshold of P<0.05 after FDR correction for multiple comparisons. Red and blue voxels represent, respectively, significant positive or inverse correlations of SRS Awareness scores with rCBF values in the ASD group. Highlighted slices (with their z-level Talairach coordinates) are those displayed in Figure 1 of the main text.

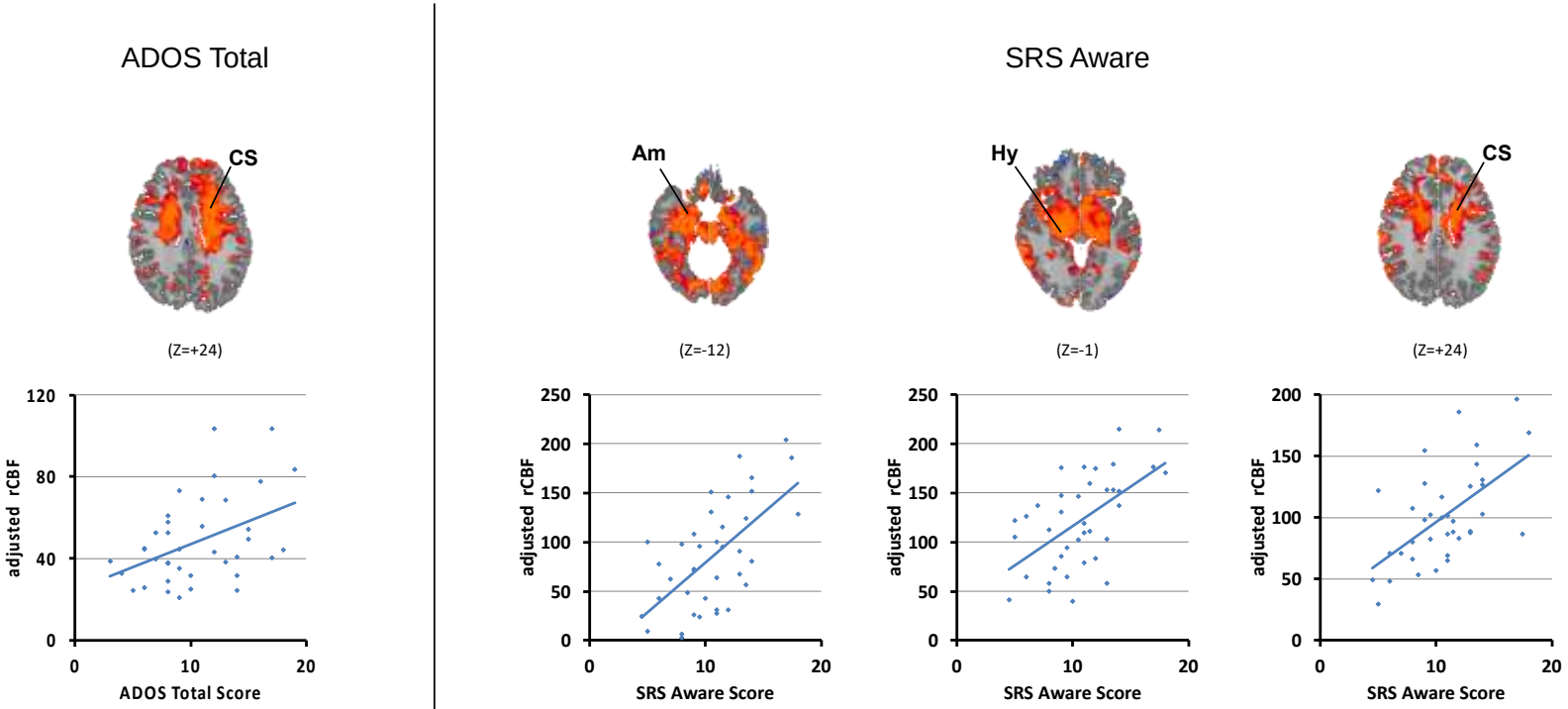

Supplementary Figure S5. Scatterplots for the Correlations of rCBF with ADOS Total and SRS Awareness Scores

These are shown for representative regions indicated above each plot in the statistical map in slices selected from the statistical maps representing the correlation of rCBF with ADOS Total or SRS Awareness scores. The line leading from the regional label to the image indicates the voxels with the images that were sampled to generate the data shown in the scatterplots. The effects of age and sex are partialed out of the rCBF values (hence the negative values for adjusted rCBF values on the y-axis. The scatterplots show that the data are well distributed around the regression lines.

Supplemental Materials Section 3b:
Age Effects Showing All Slices

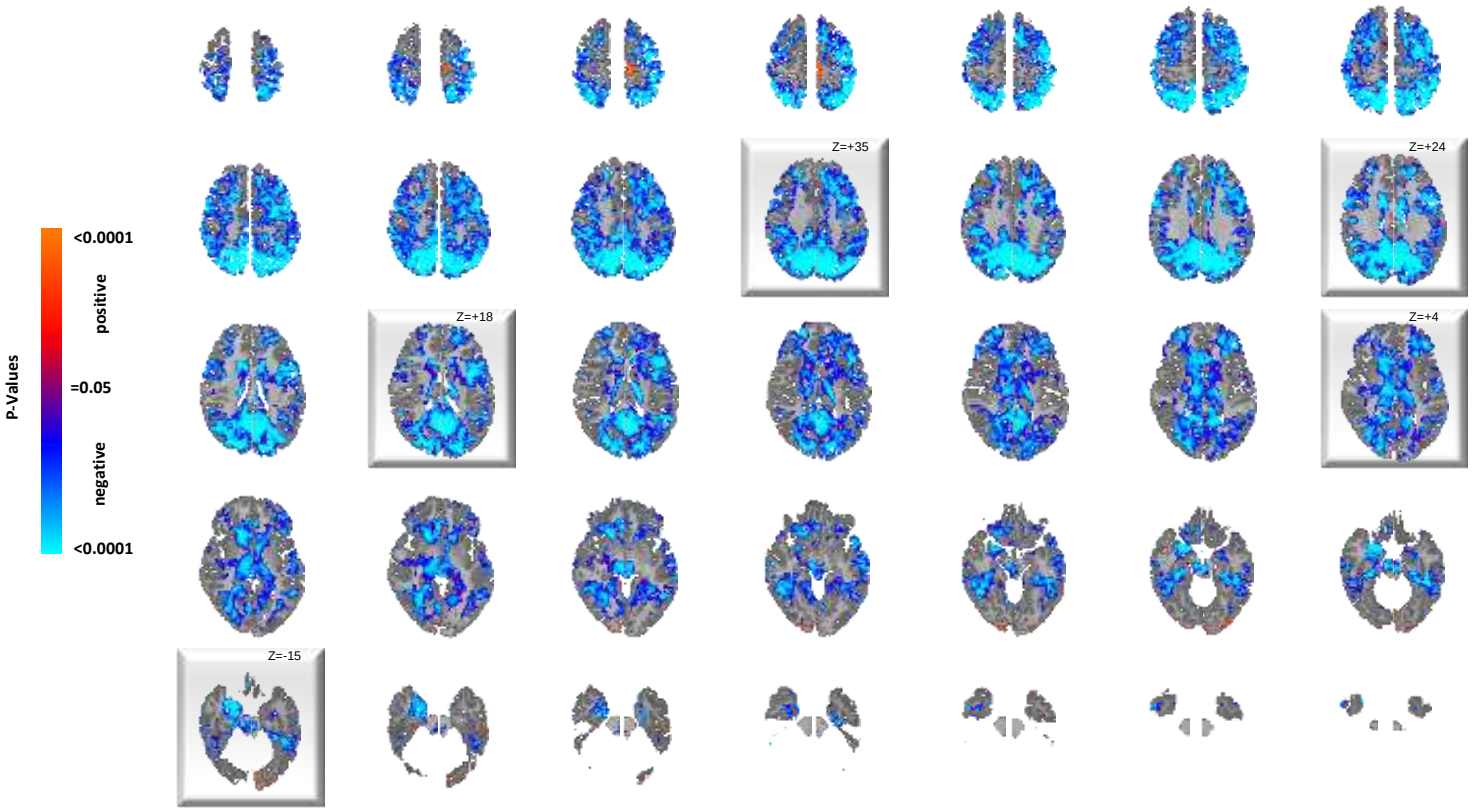

Supplementary Figure S6. Correlates of rCBF with Age in the TD Group Only for All Slices

This map shows the significance of age correlations with resting rCBF at each voxel in the TD group, while covarying for sex, in all slices. Red and blue voxels represent, respectively, significant positive or inverse correlations of age with rCBF values. Highlighted slices (with their z-level Talairach coordinates) are those displayed in Figure 2 of the main text.

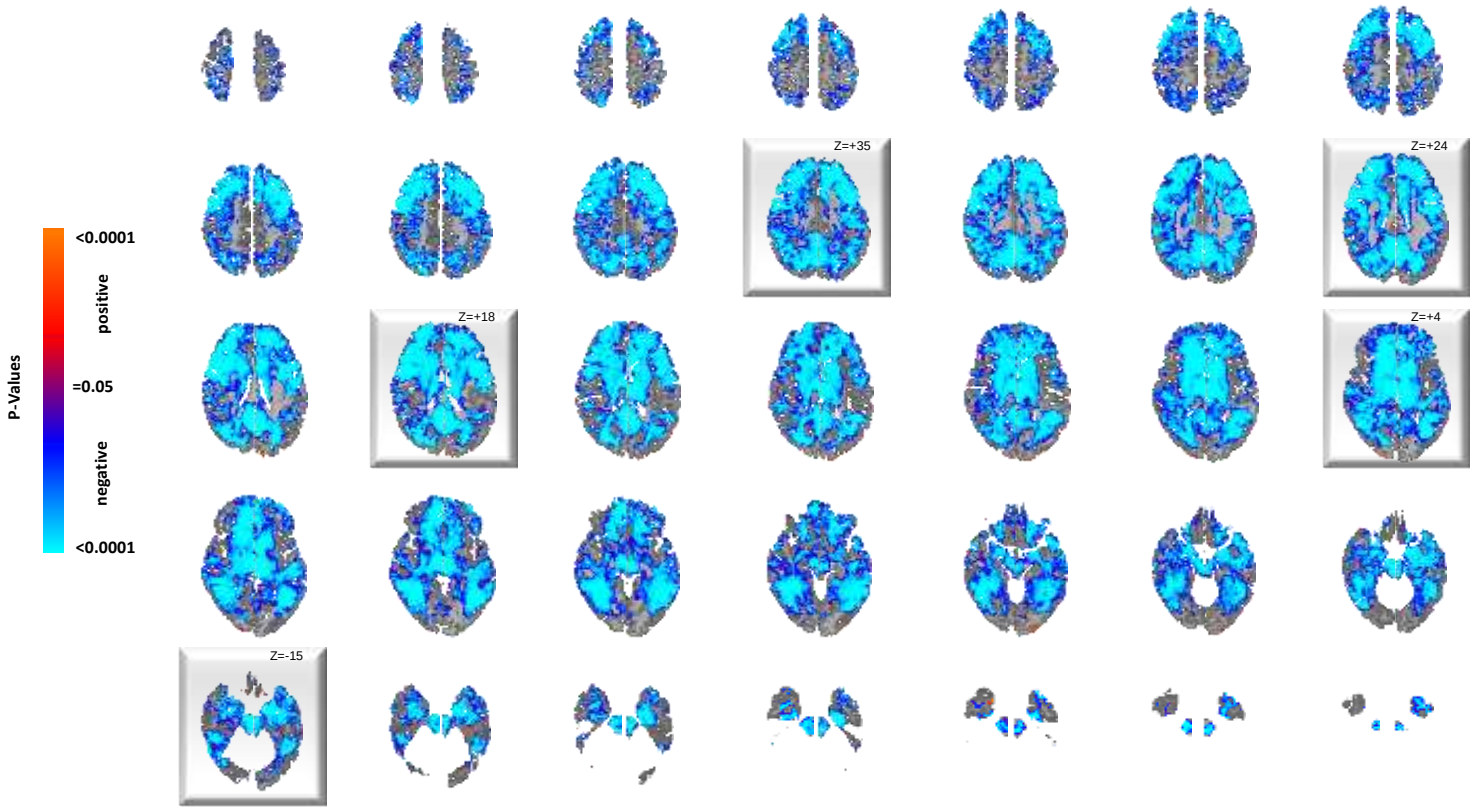

Supplementary Figure S7. Correlates of rCBF with Age in the ASD Group Only for All Slices

This map shows the significance of age correlations with resting rCBF at each voxel in the ASD group, while covarying for sex, in all slices. Red and blue voxels represent, respectively, significant positive or inverse correlations of age with rCBF values. Highlighted slices (with their z-level Talairach coordinates) are those displayed in Figure 2 of the main text.

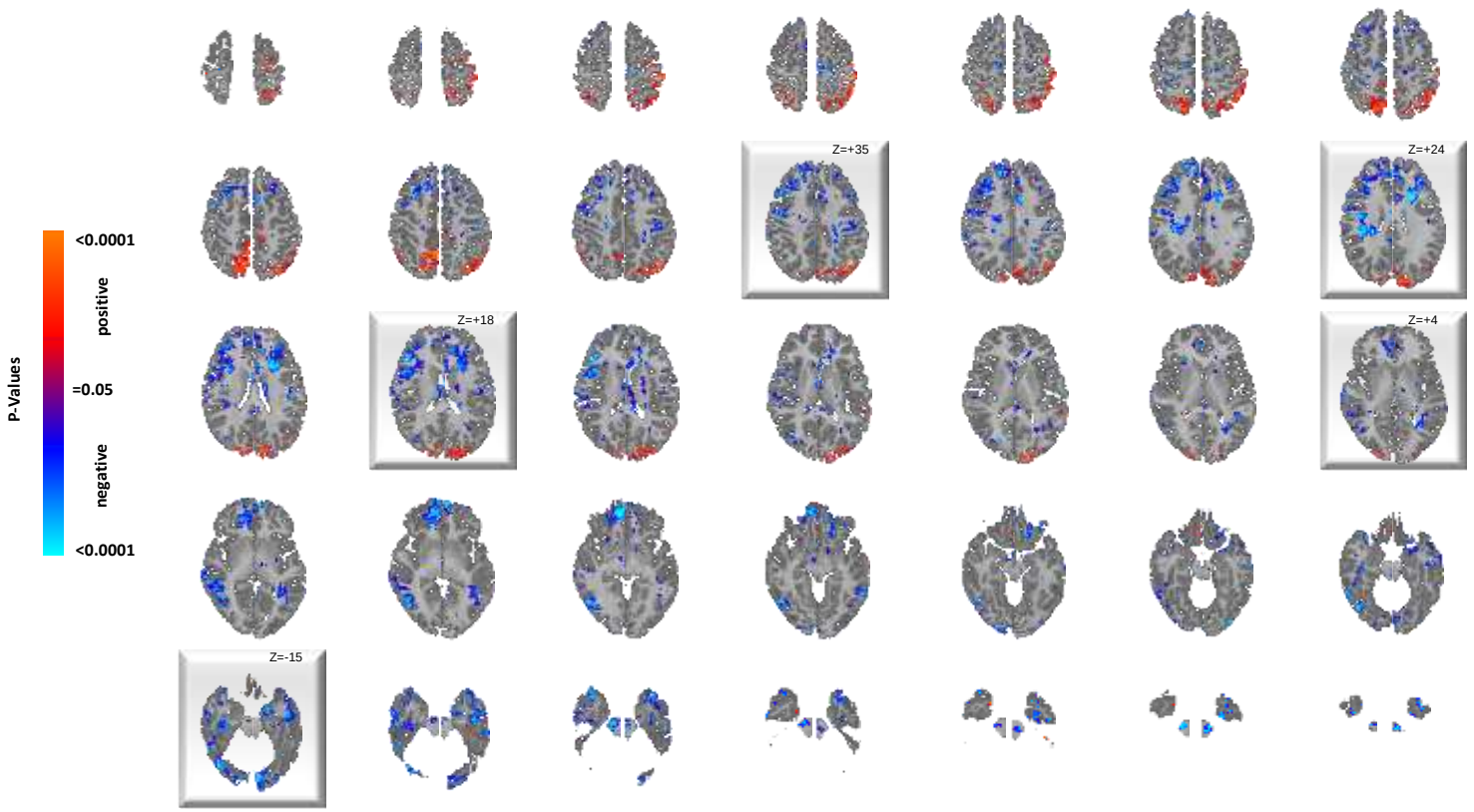

Supplementary Figure S8. The Interaction of Diagnosis with Age in All Slices

This map shows the significant effects of the interaction of age with diagnosis (ASD or TD) on rCBF at each voxel in all slices, while covarying for sex and including the main effects of age and diagnosis in a hierarchically well formulated statistical model. The interaction effect indicates voxels where the correlation of age with rCBF differs significantly across the ASD and TD groups. Red and blue voxels represent the mathematical sign (positive or negative, respectively) of the F-test statistic for the interaction. Highlighted slices (with their z-level Talairach coordinates) are those displayed in Figure 2 of the main text.

Supplemental Materials Section 3c:
Sex Effects Showing All Slices

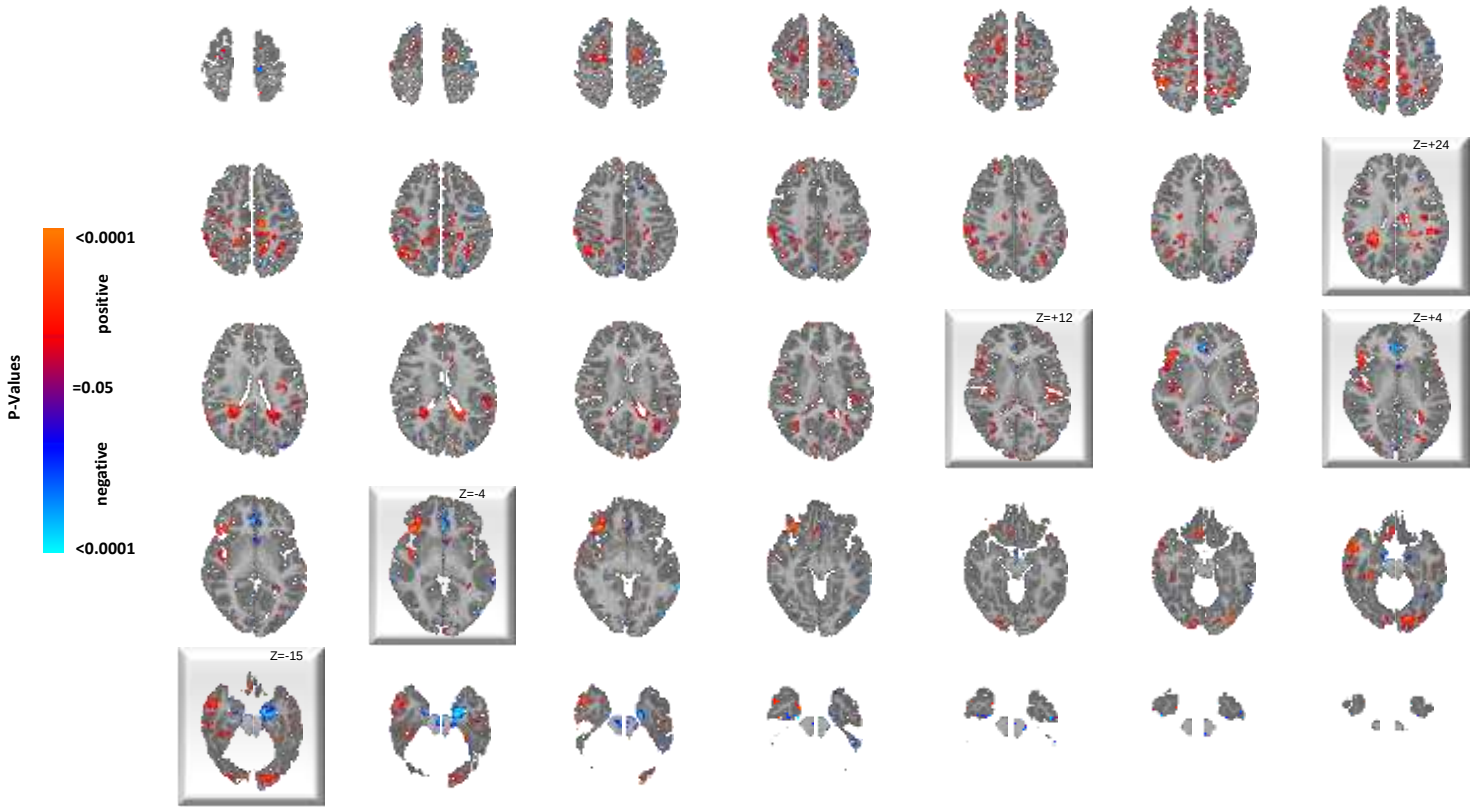

Supplementary Figure S9. Sex Differences in rCBF within the TD Group Only for All Slices

This shows all maps illustrating the significance of sex correlations with resting rCBF at each voxel in the TD group in all slices, while covarying for age. Red and blue voxels represent significantly larger rCBF values in males or females, respectively. Shown here are all slices for which data was collected in the brain. Highlighted slices (with their z-level Talairach coordinates) are those displayed in Figure 2 of the main text.

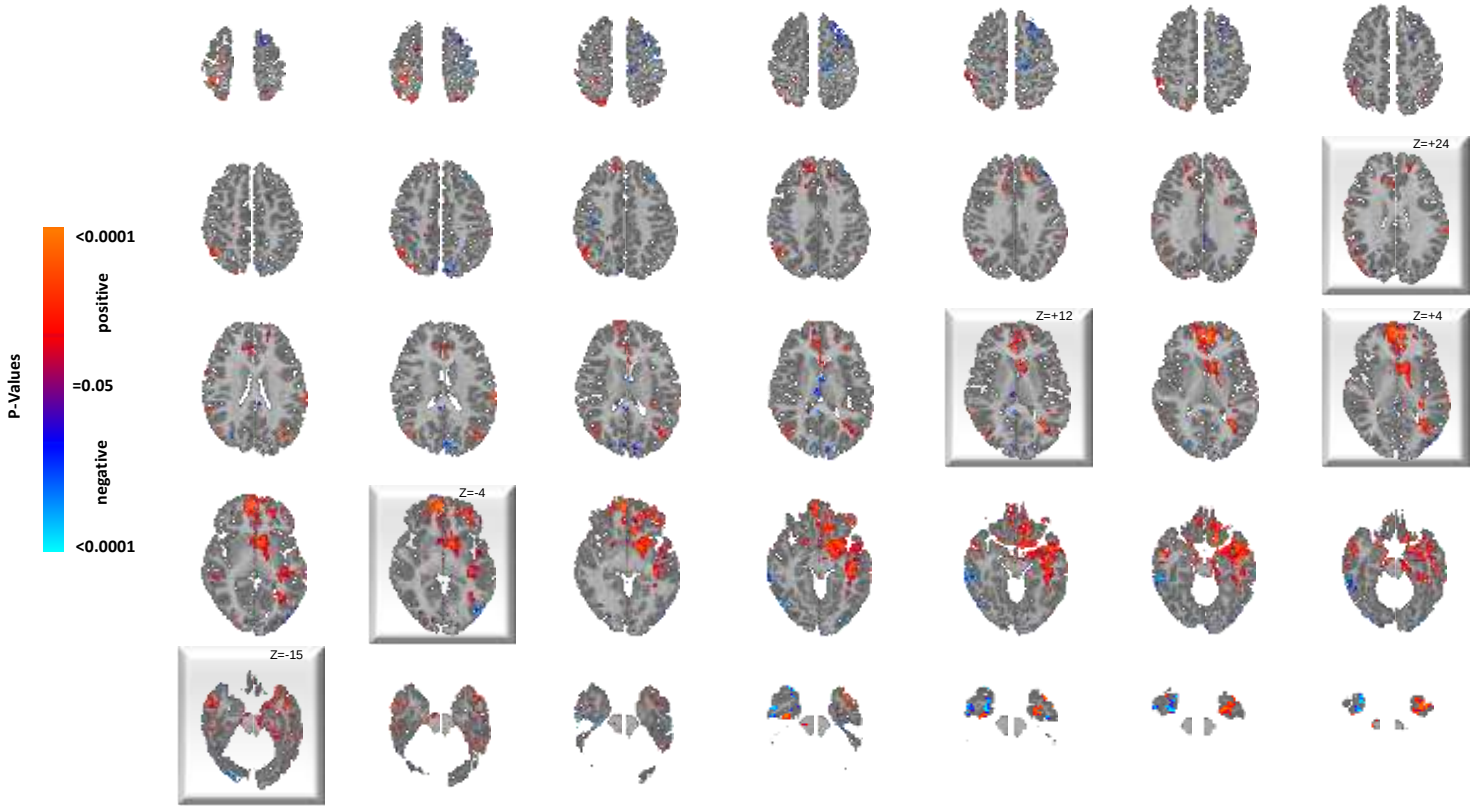

Supplementary Figure S10. Sex Differences in rCBF within the ASD Group Only for All Slices

This shows all maps illustrating the significance of sex correlations with resting rCBF at each voxel in the ASD group in all slices, while covarying for age. Red and blue voxels represent significantly larger rCBF values in males or females, respectively. Shown here are all slices for which data was collected in the brain. Highlighted slices (with their z-level Talairach coordinates) are those displayed in Figure 2 of the main text.

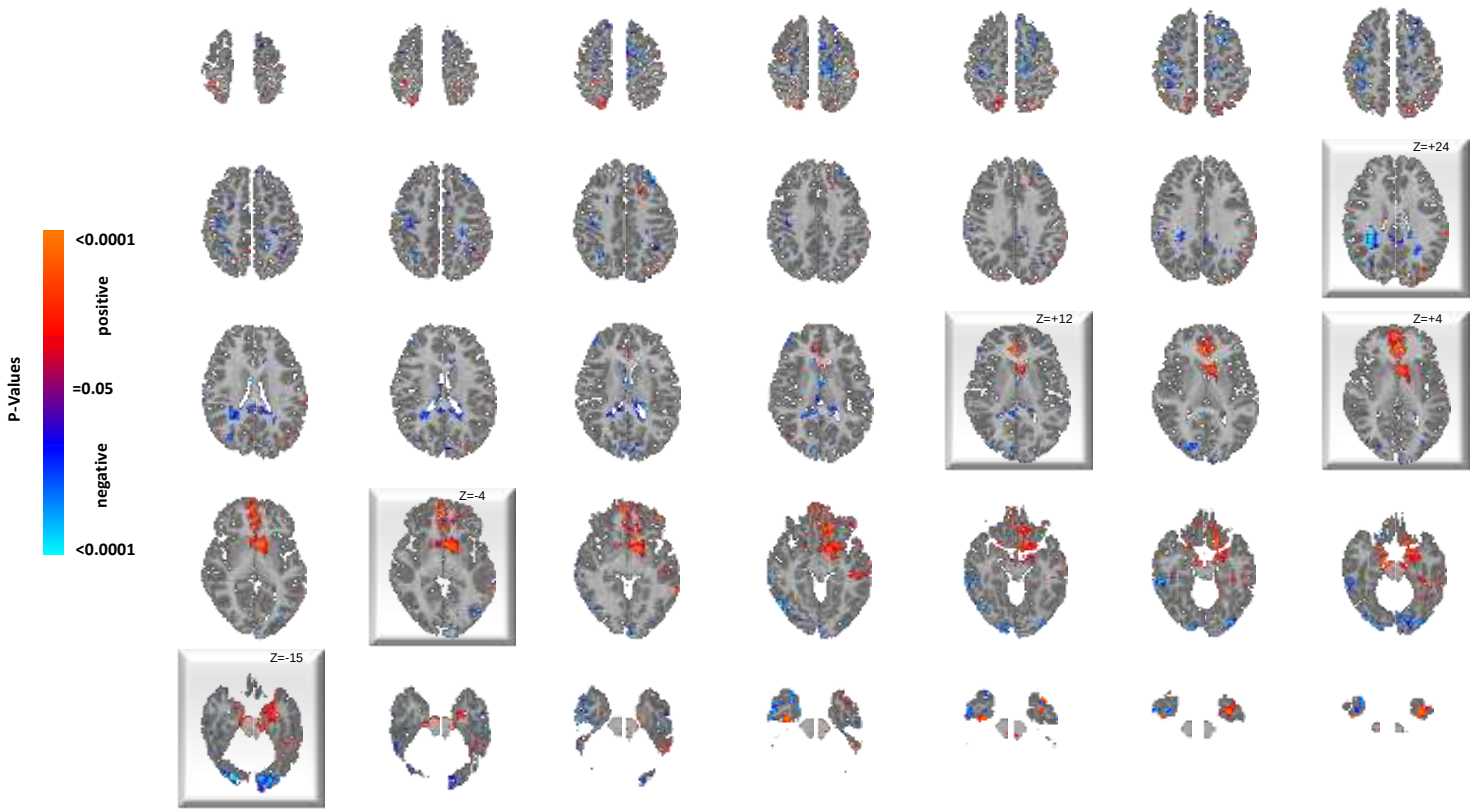

Supplementary Figure S11. The Interaction of Diagnosis with Sex in All Slices

This map shows the significant interaction effects of sex (male or female) with diagnosis (ASD or TD) on rCBF at each voxel in all slices, while covarying for age and including the main effects of sex and diagnosis in a hierarchically well formulated statistical model. The interaction effect indicates voxels where the correlation of age with rCBF differs significantly across the ASD and TD groups. Red and blue voxels represent the mathematical sign (positive or negative, respectively) of the F-test statistic for the interaction. Highlighted slices (with their z-level Talairach coordinates) are those displayed in Figure 2 of the main text.

Supplemental Materials Section 3d:
FSIQ Effects Showing All Slices

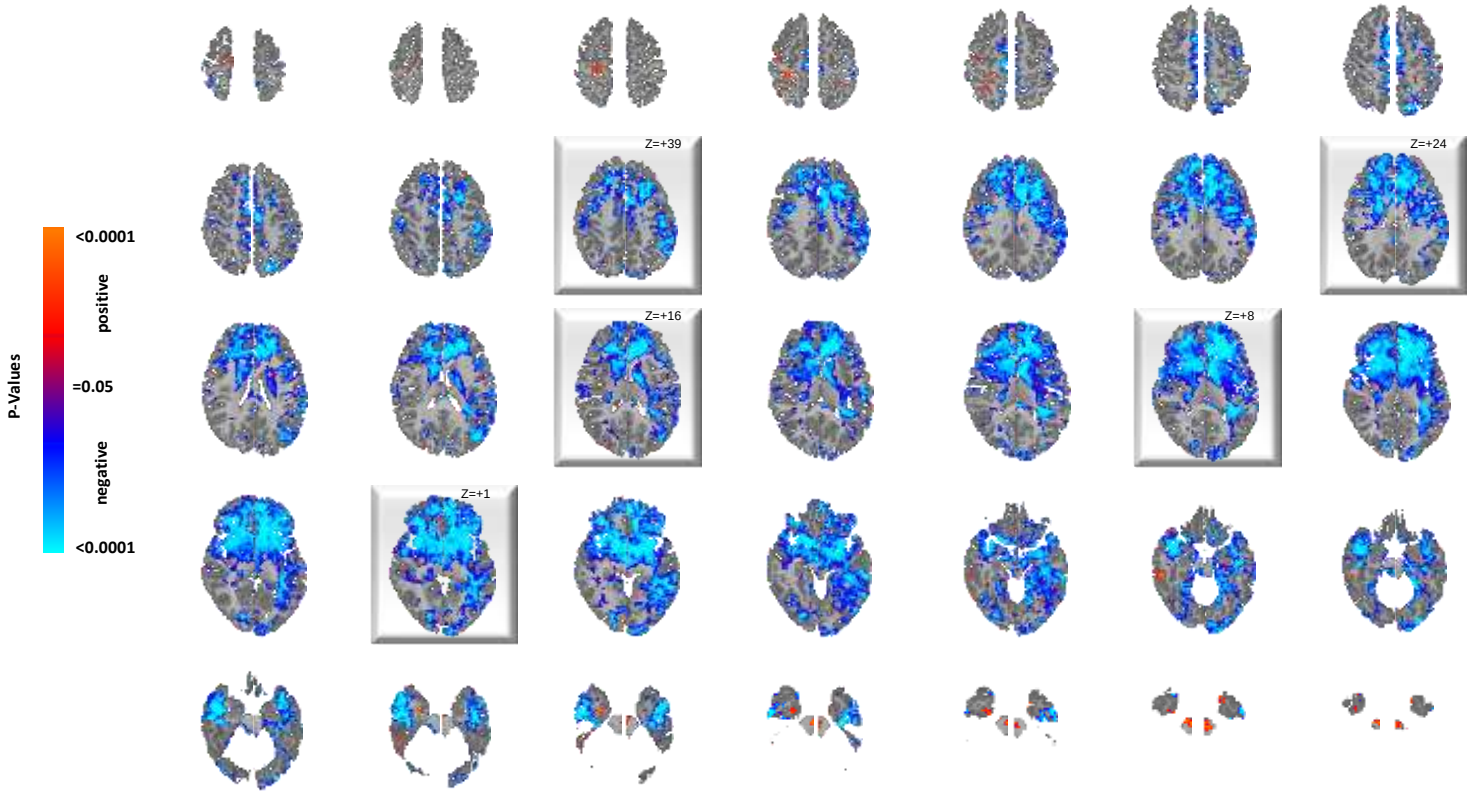

Supplementary Figure S12. Correlates of rCBF with FSIQ in the TD Group Only for All Slices

This shows all maps illustrating the significance of FSIQ correlations with resting rCBF at each voxel in the TD group in all slices, while covarying for age and sex. Red and blue voxels represent, respectively, significant positive or inverse correlations of FSIQ with rCBF values. Highlighted slices (with their z-level Talairach coordinates) are those displayed in Figure 2 of the main text.

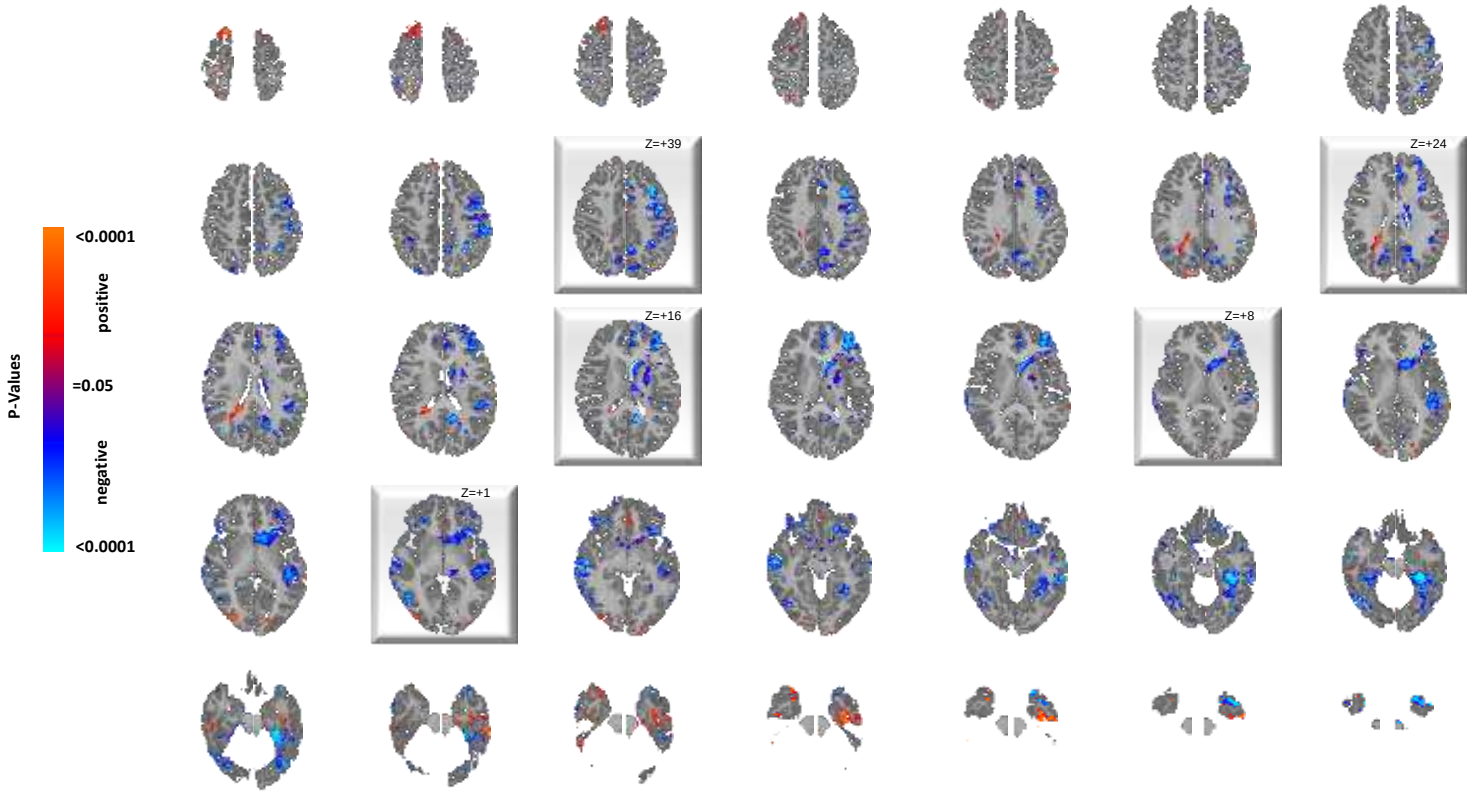

Supplementary Figure S13. Correlates of rCBF with FSIQ in the ASD Group Only for All Slices
This shows all maps illustrating the significance of FSIQ correlations with resting rCBF at each voxel in the ASD group in all slices, while covarying for age and sex. Red and blue voxels represent, respectively, significant positive or inverse correlations of FSIQ with rCBF values. Highlighted slices (with their z-level Talairach coordinates) are those displayed in Figure 2 of the main text.

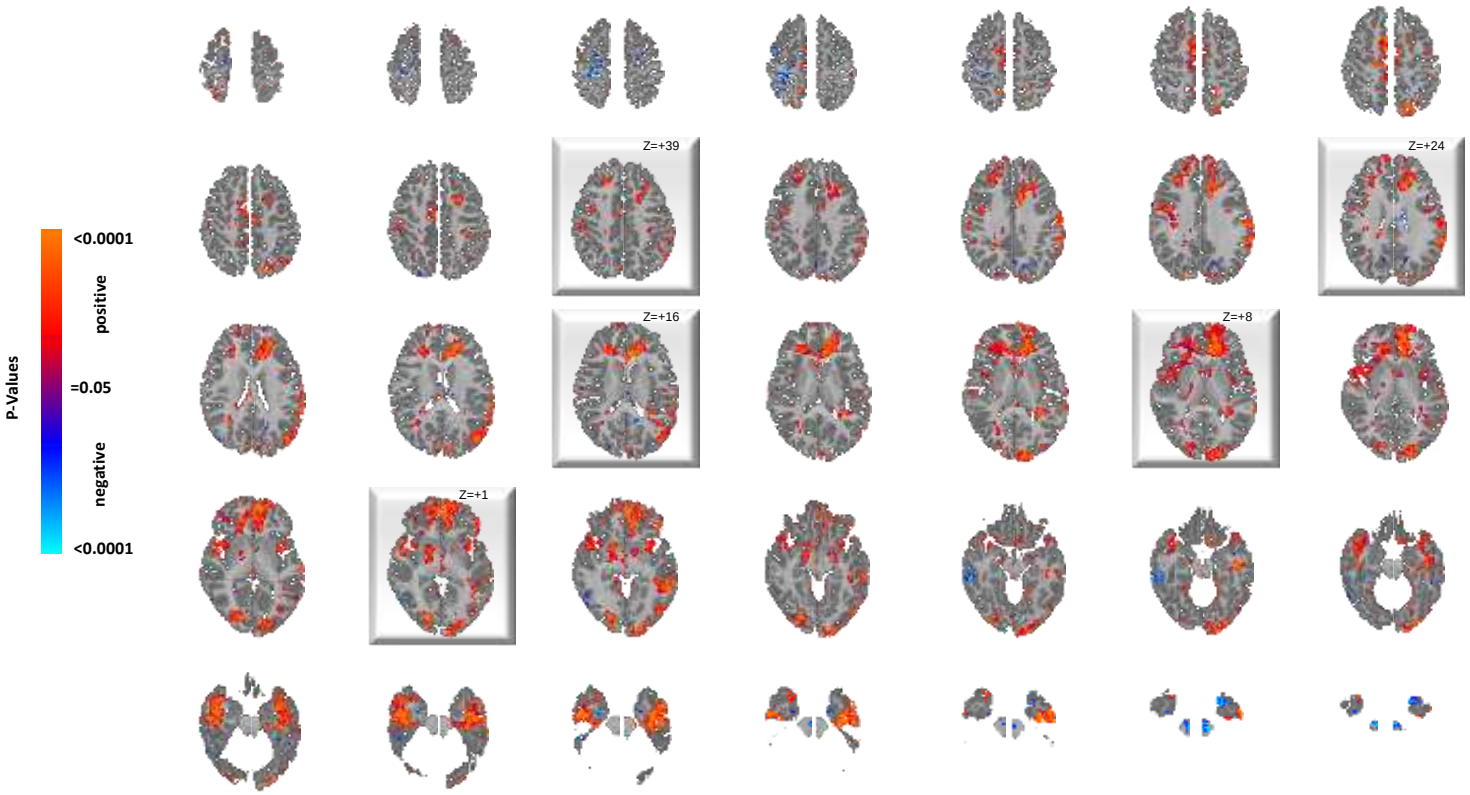

Supplementary Figure S14. The Interaction of Diagnosis with FSIQ in All Slices

This map shows the significant interaction effects of FSIQ with diagnosis (ASD or TD) on rCBF at each voxel in all slices, while covarying for age and sex and including the main effects of FSIQ and diagnosis in a hierarchically well formulated statistical model. The interaction effect indicates voxels where the correlation of FSIQ with rCBF differs significantly across the ASD and TD groups. Red and blue voxels represent the mathematical sign (positive or negative, respectively) of the F-test statistic for the interaction. Highlighted slices (with their z-level Talairach coordinates) are those displayed in Figure 2 of the main text.

Supplemental Materials Section 3e:
Correlations of rCBF with NAA Metabolite Concentrations

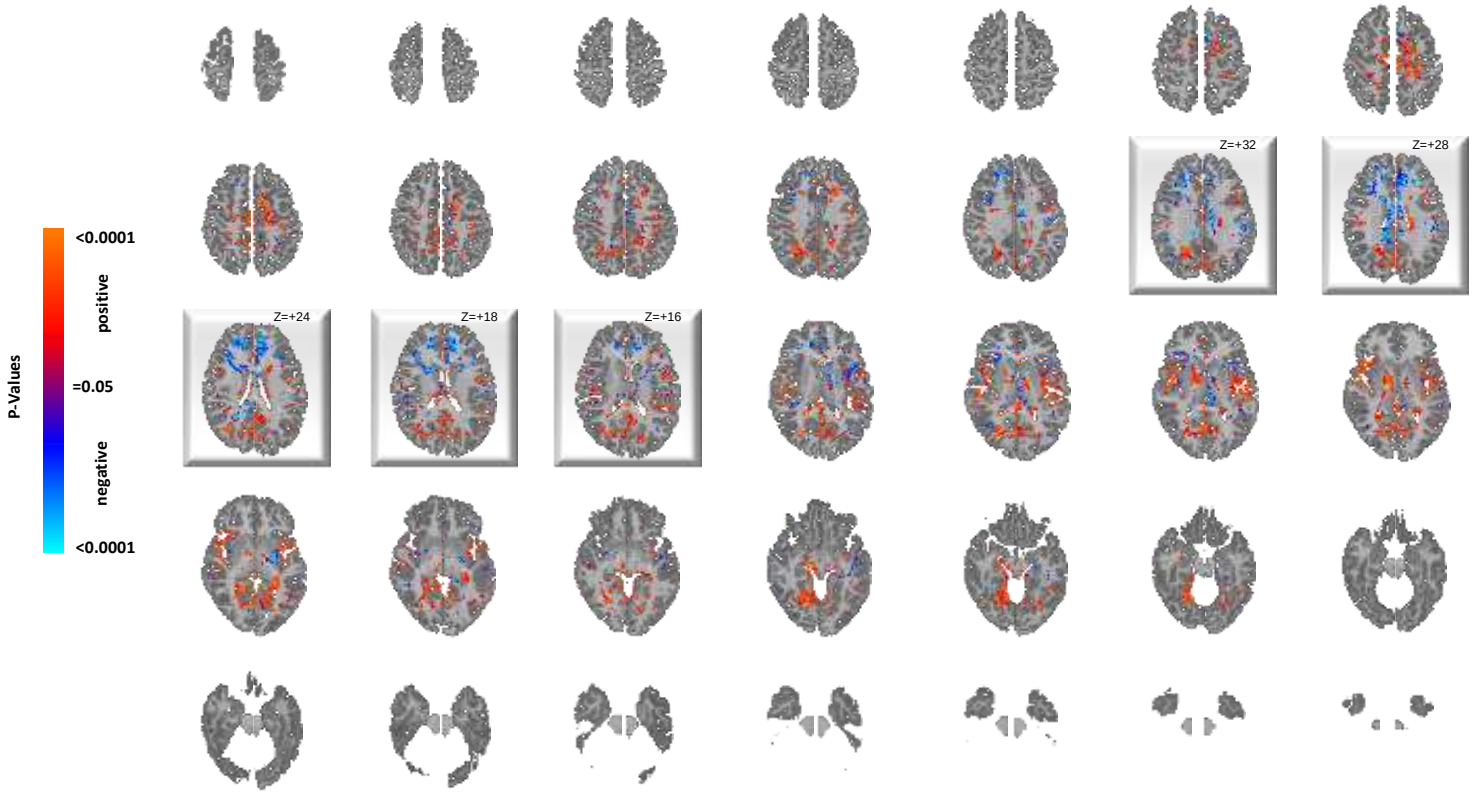

Supplementary Figure S15. Voxelwise Correlation of rCBF with NAA Concentrations in the TD Group Only in All Slices
Shown here are the voxel-wise correlations of NAA concentration with rCBF in the TD group (N=63, 48 males, 15 females, mean age 22.3 years) in all slices, while covarying for age and sex. Significance levels are FDR-corrected for the number of statistical comparisons. Red and blue voxels represent, respectively, significant positive or inverse correlations of NAA levels with rCBF values. Highlighted slices (with their z-level Talairach coordinates) are those displayed in Figure 3 of the main text.

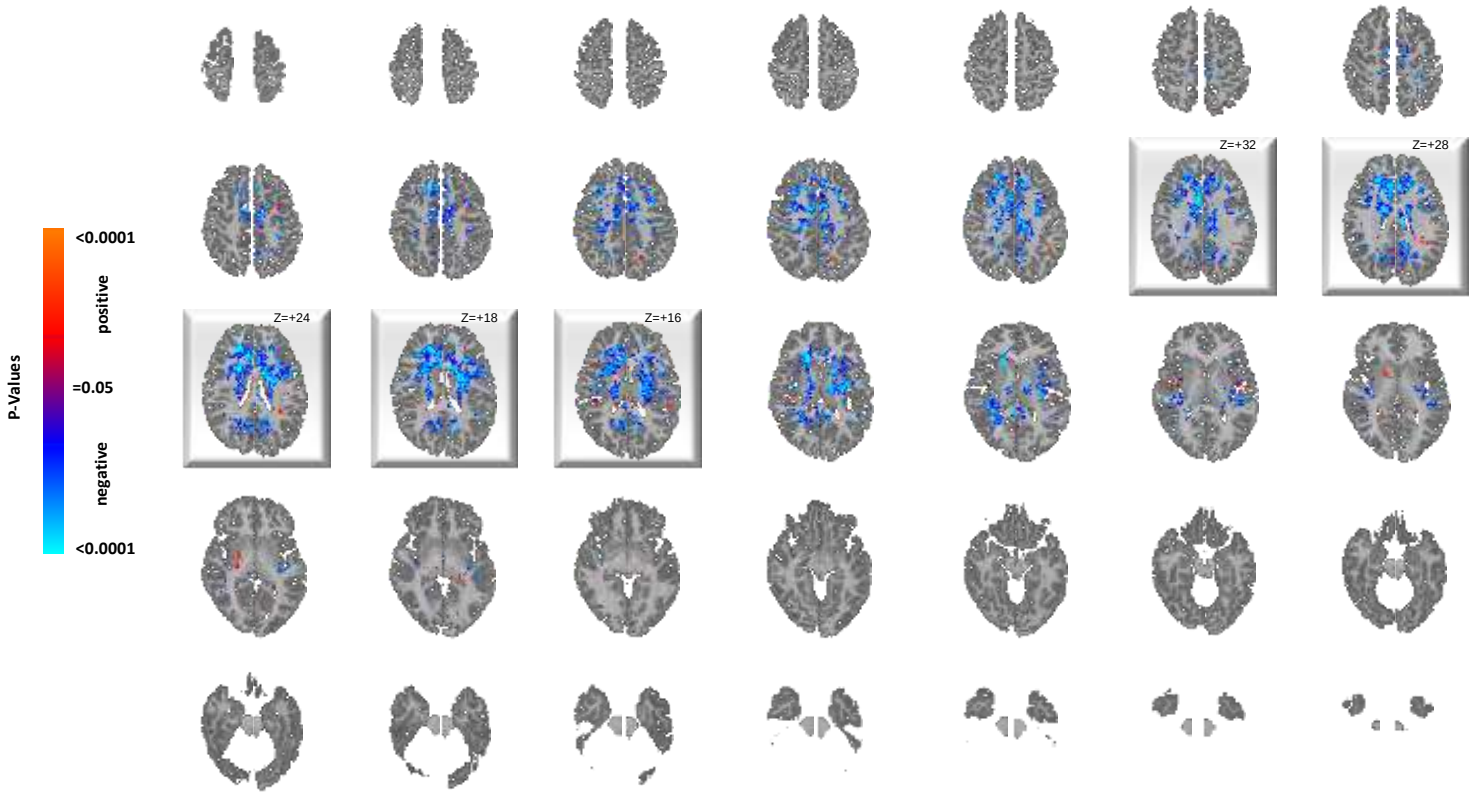

Supplementary Figure S16. Voxelwise Correlation of rCBF with NAA Concentrations in the ASD Group Only in All Slices
Shown here are the voxel-wise correlations of NAA concentration with rCBF in the ASD group (N=36, 29 males, 7 females, mean age 25.6 years) group in all slices, while covarying for age and sex. Significance levels are FDR-corrected for the number of statistical comparisons. Red and blue voxels represent, respectively, significant positive or inverse correlations of NAA levels with rCBF values. Highlighted slices (with their z-level Talairach coordinates) are those displayed in Figure 3 of the main text.

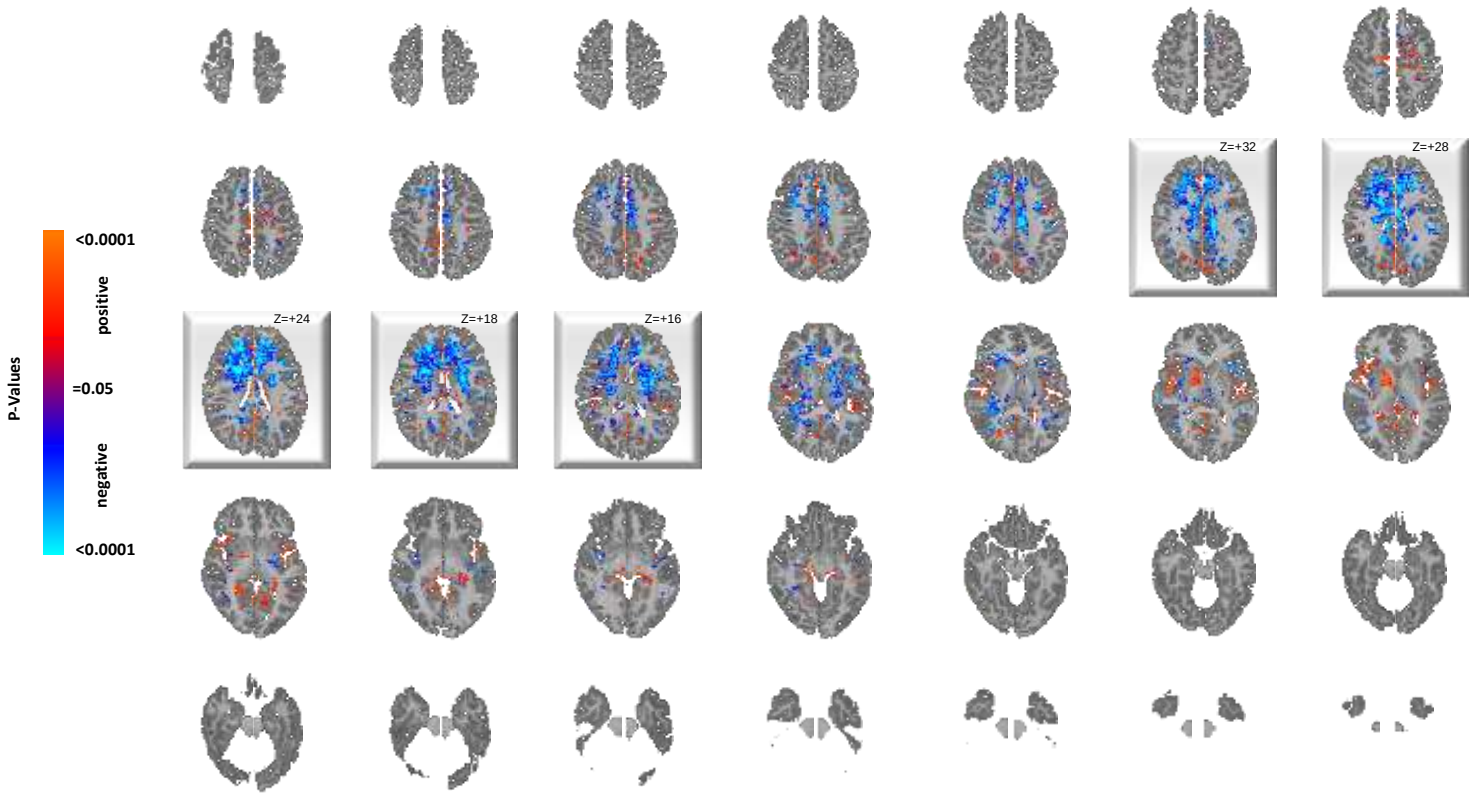

Supplementary Figure S17. Voxelwise Correlation of rCBF with NAA Concentrations in All Participants for All Slices
Shown here are the voxel-wise correlations of NAA concentration with rCBF in the ASD (N=36, 29 males, 7 females, mean age 25.6 years) and TD (N=63, 48 males, 15 females, mean age 22.3 years) groups combined in all slices, while covarying for age and sex. Significance levels are FDR-corrected for the number of statistical comparisons. Red and blue voxels represent, respectively, significant positive or inverse correlations of NAA level with rCBF values in the ASD group compared to the TD group. Highlighted slices (with their z-level Talairach coordinates) are those displayed in Figure 3 of the main text.

Supplemental Materials Section 3f:
Correlations of rCBF with Detectable Lactate

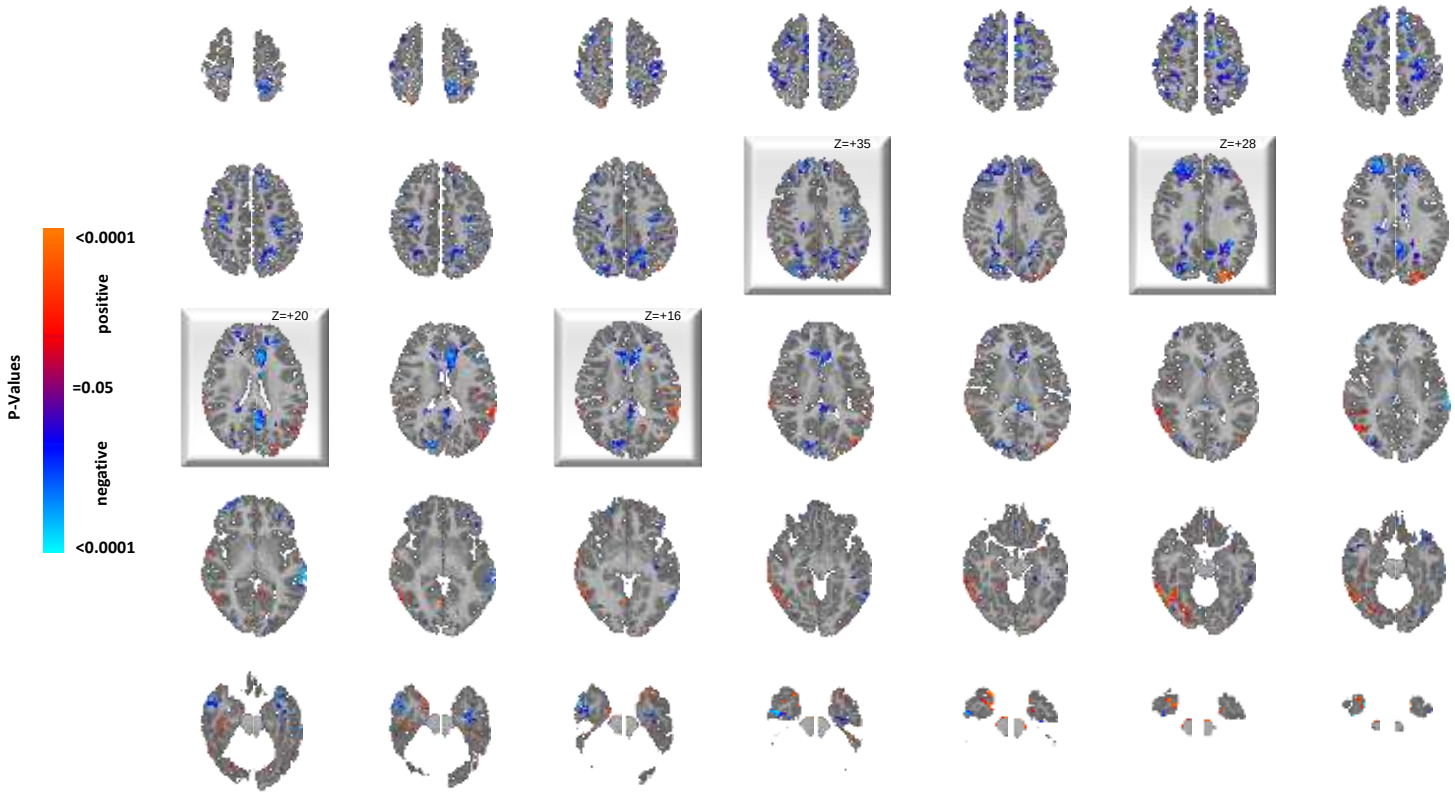

Supplementary Figure S18. rCBF in ASD Participants with or without Detectable Lactate for All Slices

This map shows all slices for the voxel-wise statistical comparison of rCBF in ASD participants who had detectable lactate (N=6, __ males, __ females, mean age __ years) compared with the ASD participants who did not have detectable lactate at any voxel, while covarying for age and sex. Significance levels are FDR-corrected for the number of statistical comparisons. Red and blue voxels represent, respectively, significantly higher or lower rCBF values, respectively, in ASD participants who had detectable lactate. Highlighted slices (with their z-level Talairach coordinates) are those displayed in Figure 3 of the main text.

Supplemental Materials Section 4:
Group Average rCBF Maps

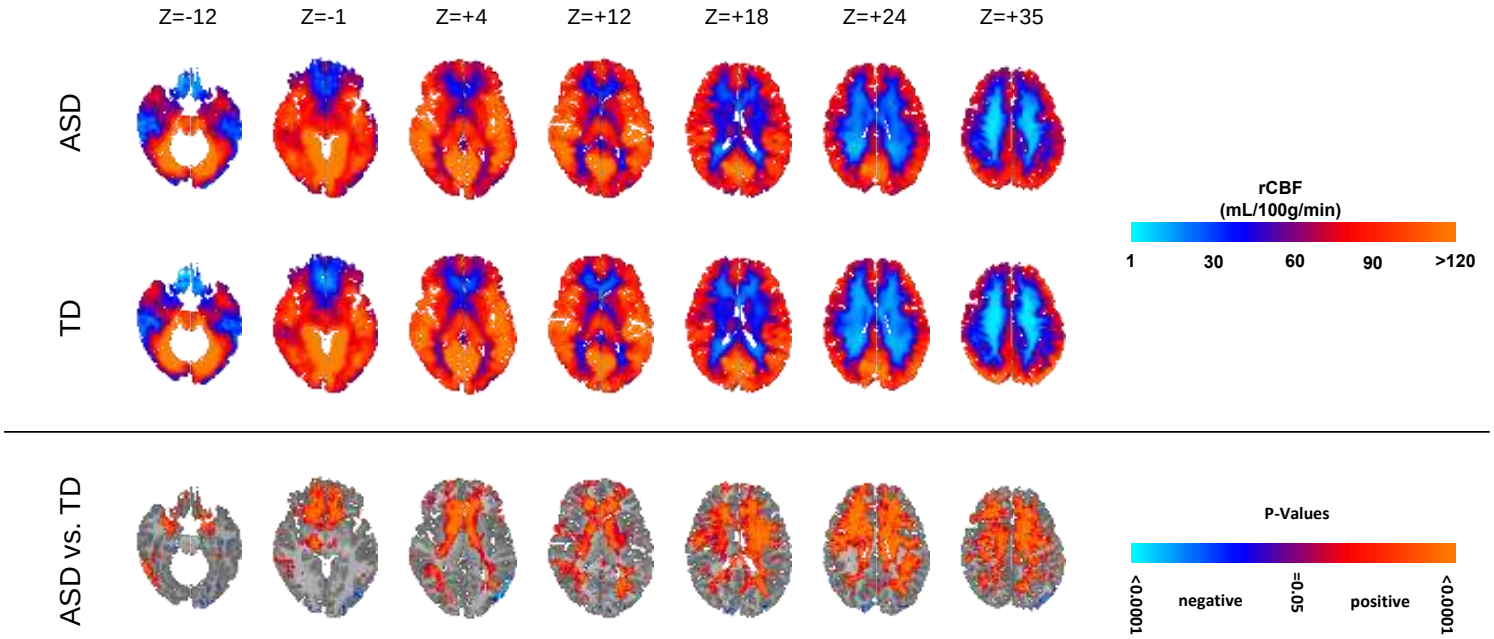

Supplementary Figure S19. Group Average Maps Contributing to Significant Group Differences in rCBF in Representative Slices
Top Row: This is a map showing the group average rCBF at each voxel in the ASD group only, partialing out the effects of age and sex, for the slices shown in Figure 1 of the main text.
Middle Row: This is a map showing the group average rCBF at each voxel in the TD group only, partialing out the effects of age and sex, for the slices shown in Figure 1 of the main text.
Bottom Row: These are the statistically significant group differences (ASD vs TD) in rCBF while covarying for age and sex, displayed at a threshold of $P<0.05$ after correction for multiple comparisons, for the slices shown in Figure 1 of the main text.

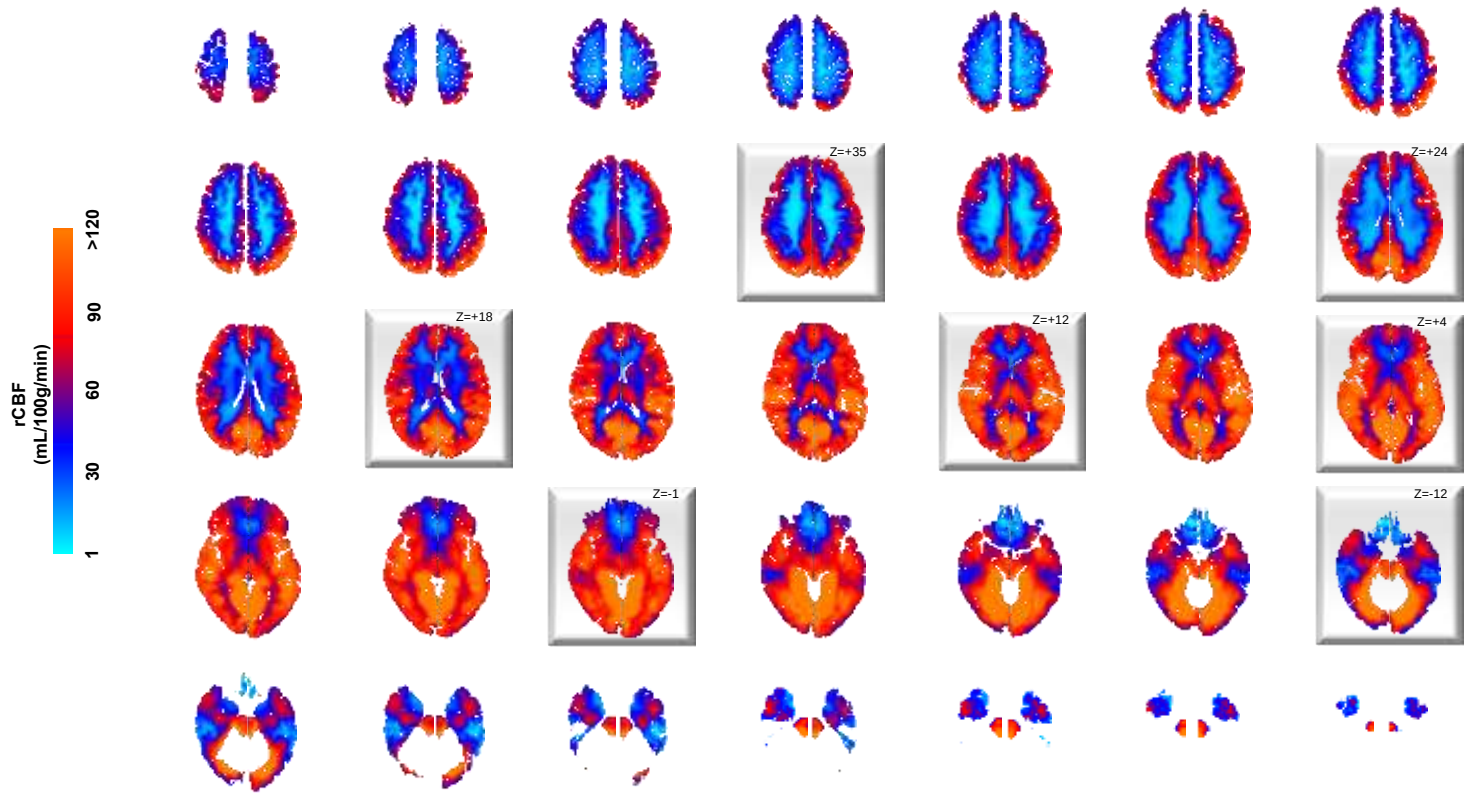

Supplementary Figure S20. Average Perfusion in the TD Group in All Slices
This is a map showing the group average rCBF at each voxel in all slices in the TD group only, partialing out the effects of age and sex.

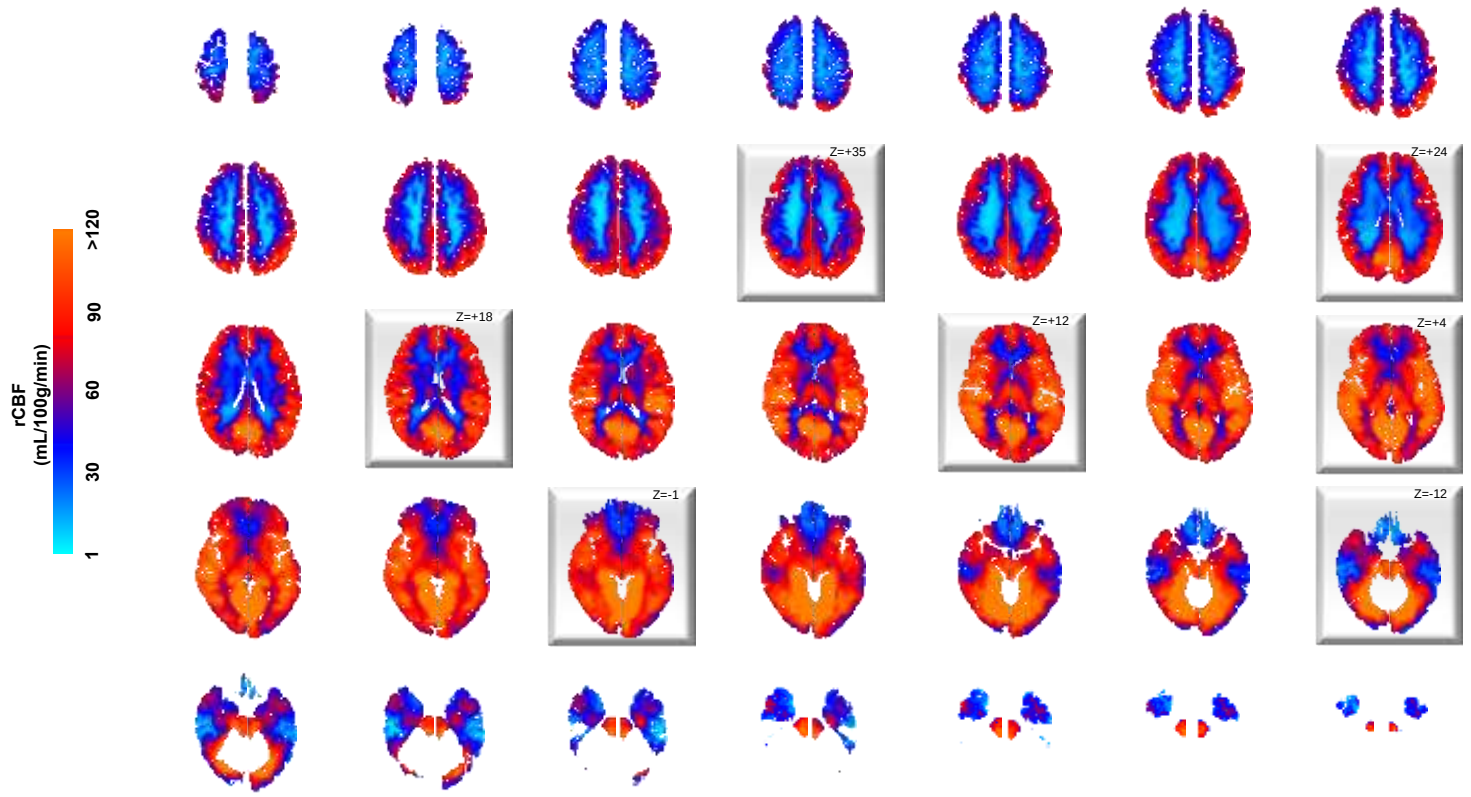

Supplementary Figure S21. Average Perfusion in the ASD Group in All Slices
This is a map showing the group average rCBF at each voxel in all slices in the ASD group only, partialing out the effects of age and sex.

Supplemental Materials Section 5a:
rCBF Correlations with Scores in Other ADOS Symptom Domains

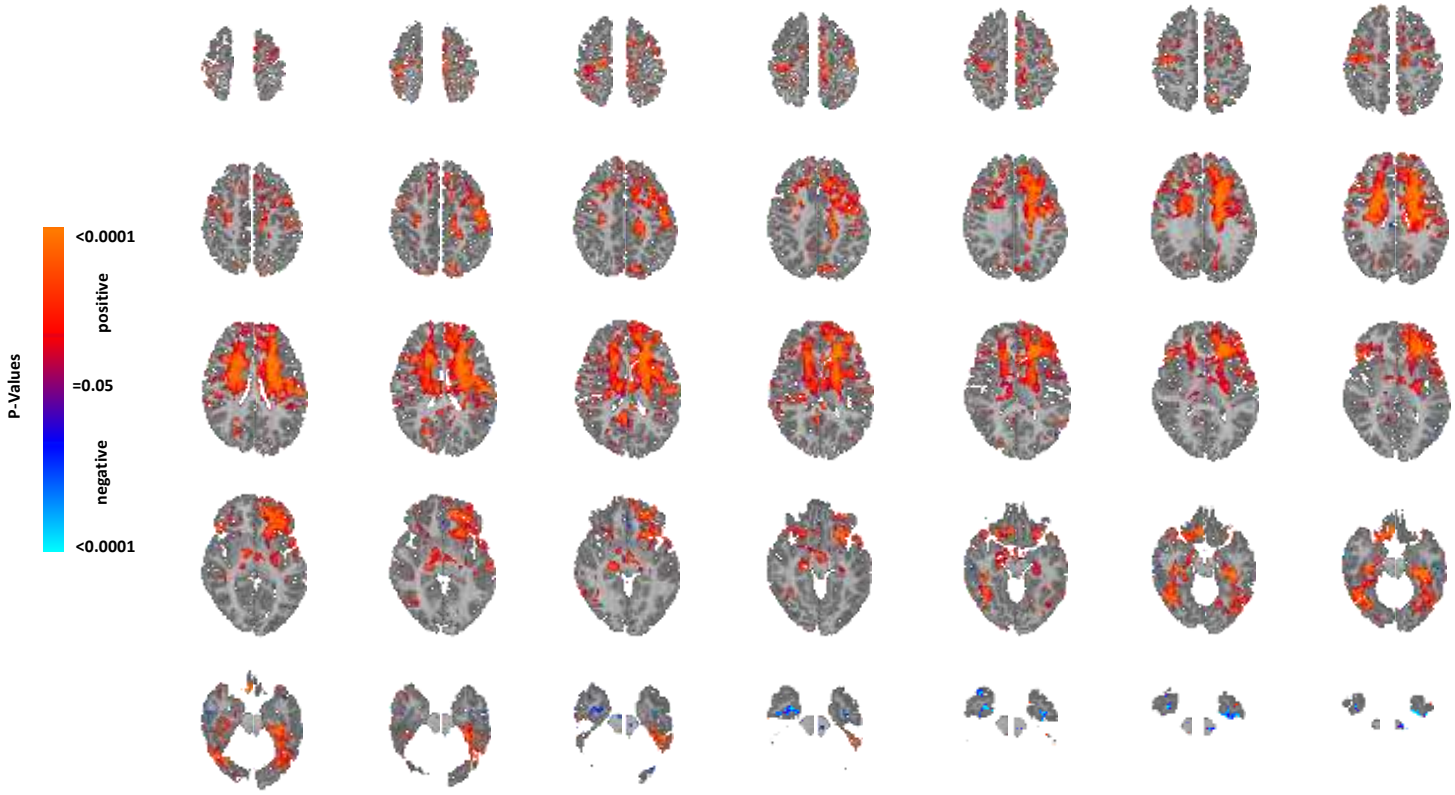

Supplementary Figure S22. Correlation of rCBF with ADOS Social Affect Scores for All Slices

This shows the statistically significant correlations of ADOS Social Affect scores with rCBF values in the ASD group for all slices while covarying for age and sex, displayed at a threshold of P<0.05 after FDR correction for multiple comparisons. Red and blue voxels represent, respectively, significant positive or inverse correlations of ADOS Social Affect scores with rCBF values in the ASD group.

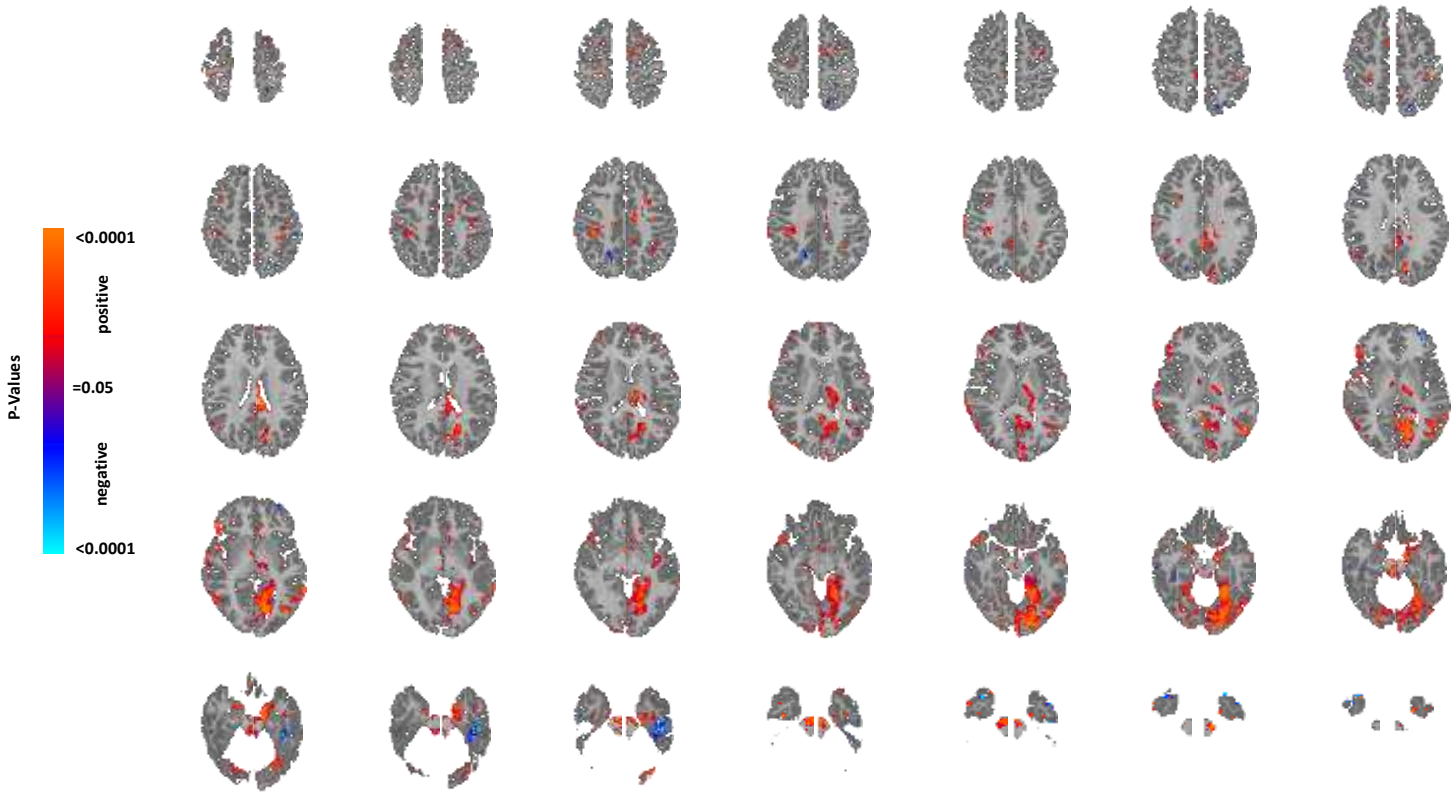

Supplementary Figure S23. Correlation of rCBF with ADOS Restrictive and Repetitive Behaviors Scores for All Slices
This shows the statistically significant correlations of ADOS Restrictive and Repetitive Behaviors scores with rCBF values in the ASD group for all slices while covarying for age and sex, displayed at a threshold of P<0.05 after FDR correction for multiple comparisons. Red and blue voxels represent, respectively, significant positive or inverse correlations of ADOS Restrictive and Repetitive Behaviors scores with rCBF values in the ASD group.

Supplemental Materials Section 5b:
SRS Symptom Domains

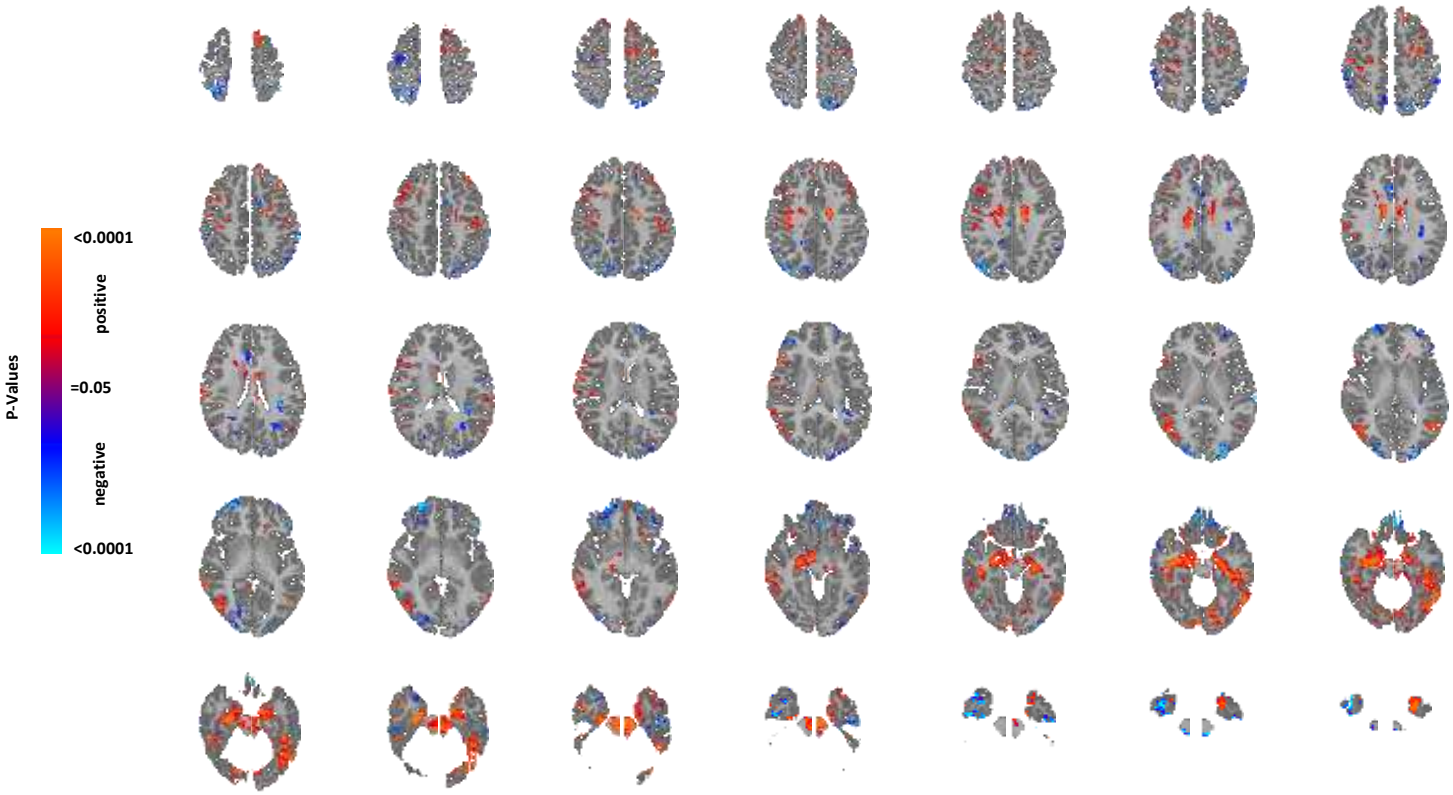

Supplementary Figure S24. Correlation of rCBF with SRS Total Scores for All Slices

This shows the statistically significant correlations of SRS Total scores with rCBF values in the ASD group for all slices while covarying for age and sex, displayed at a threshold of P<0.05 after FDR correction for multiple comparisons. Red and blue voxels represent, respectively, significant positive or inverse correlations of SRS Total scores with rCBF values in the ASD group.

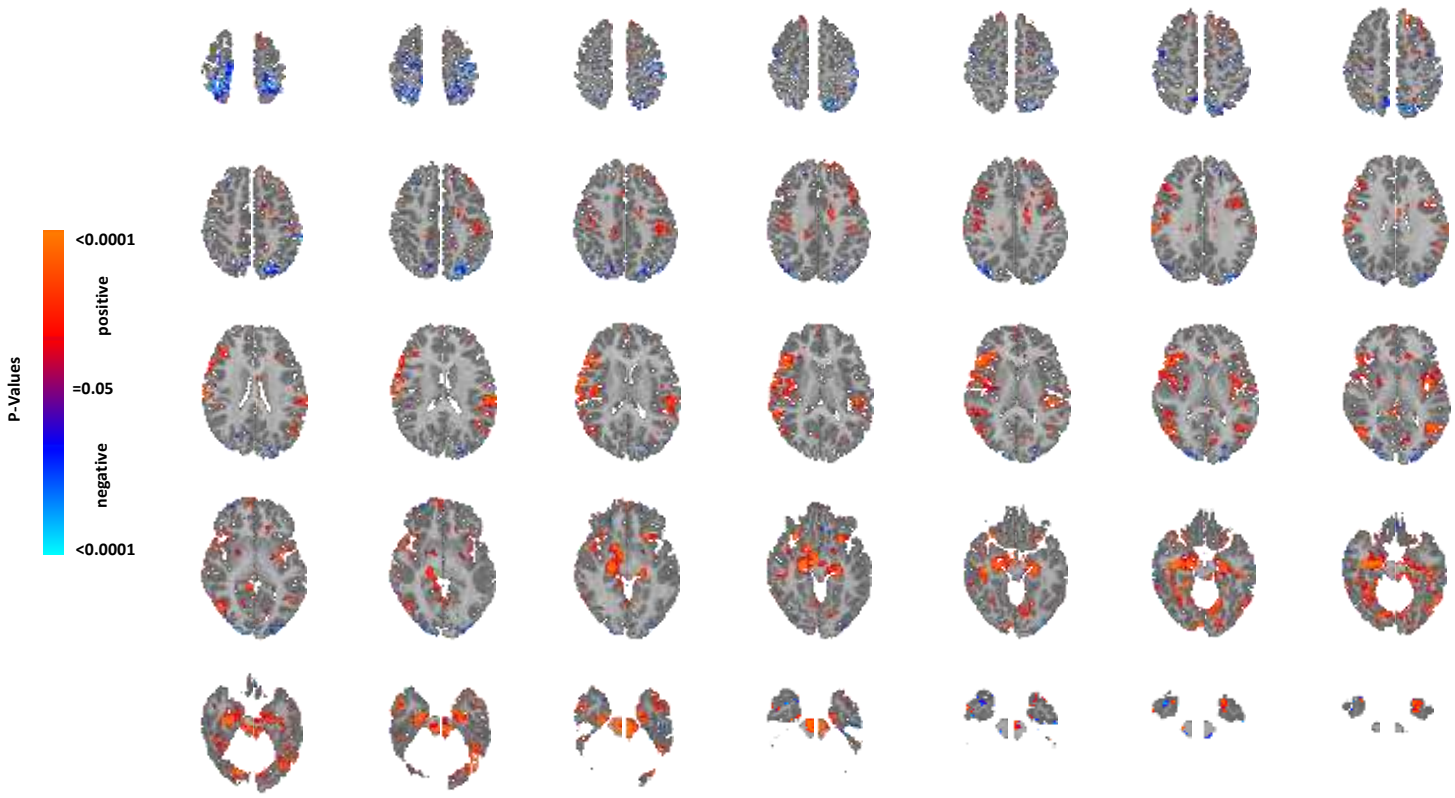

Supplementary Figure S25. Correlation of rCBF with SRS Motivation Scores for All Slices

This shows the statistically significant correlations of SRS Motivation scores with rCBF values in the ASD group for all slices while covarying for age and sex, displayed at a threshold of P<0.05 after FDR correction for multiple comparisons. Red and blue voxels represent, respectively, significant positive or inverse correlations of SRS Motivation scores with rCBF values in the ASD group.

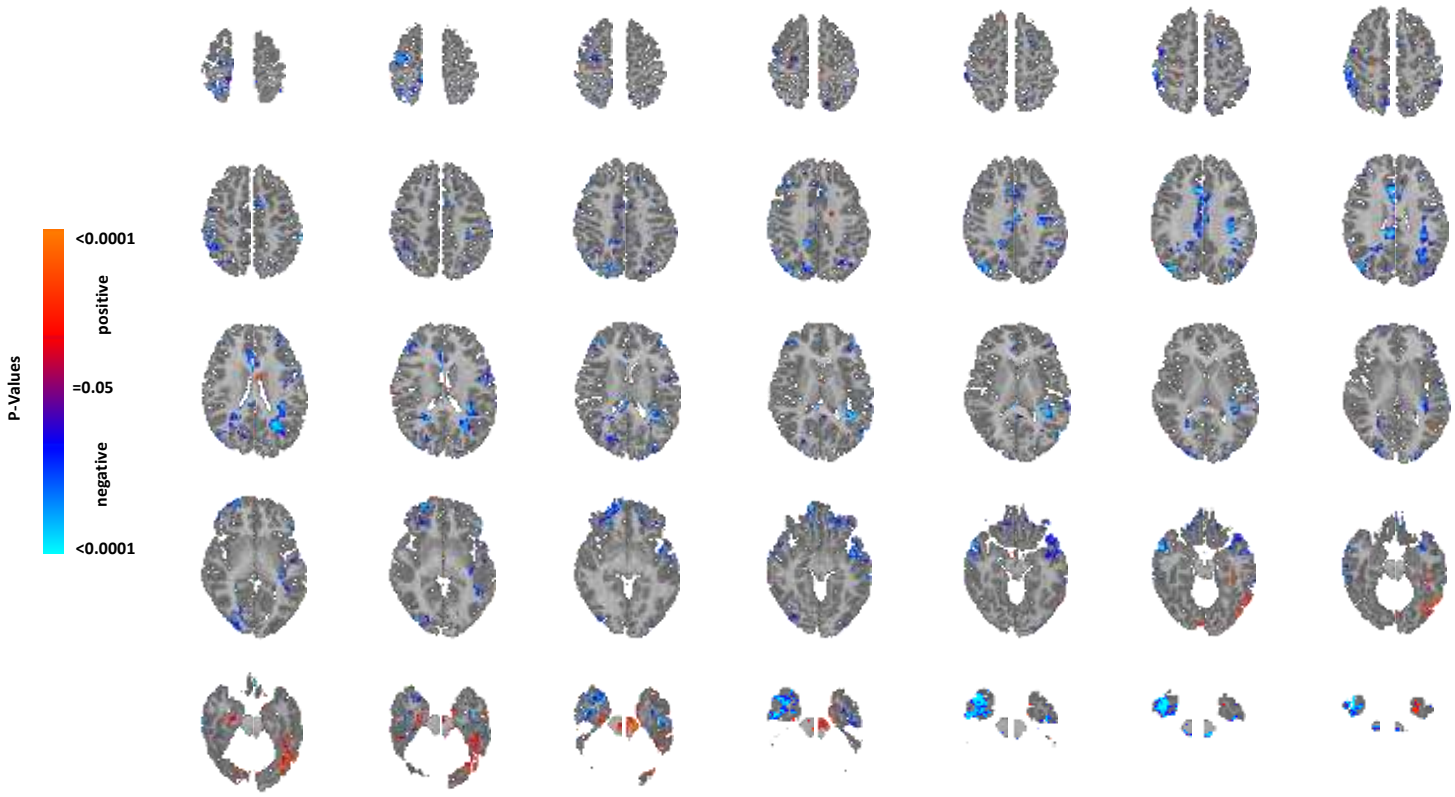

Supplementary Figure S26. Correlation of rCBF with SRS Mannerism Scores for All Slices

This shows the statistically significant correlations of SRS Mannerism scores with rCBF values in the ASD group for all slices while covarying for age and sex, displayed at a threshold of P<0.05 after FDR correction for multiple comparisons. Red and blue voxels represent, respectively, significant positive or inverse correlations of SRS Mannerism scores with rCBF values in the ASD group.

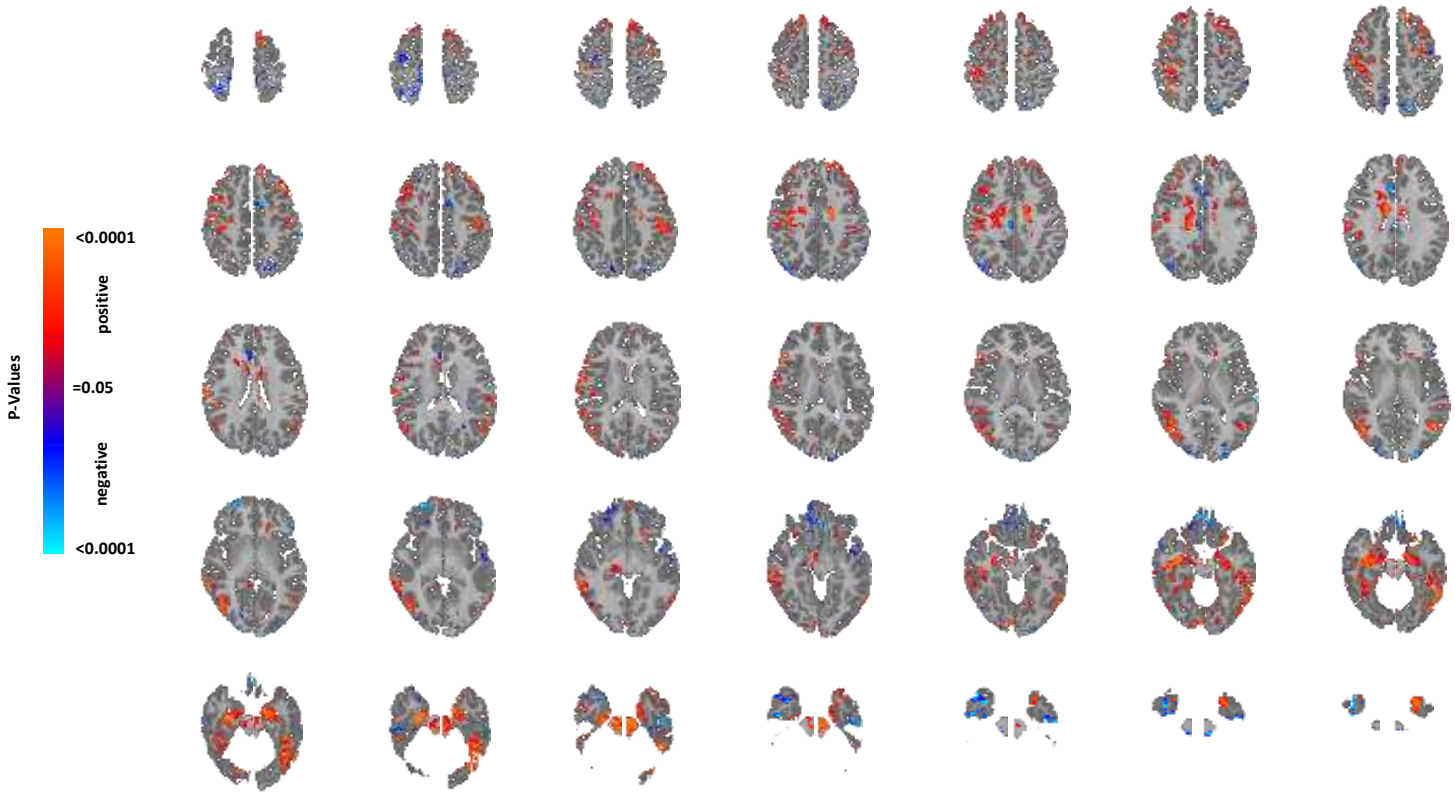

Supplementary Figure S27. Correlation of rCBF with SRS Communication Scores for All Slices
This shows the statistically significant correlations of SRS Communication scores with rCBF values in the ASD group for all slices while covarying for age and sex, displayed at a threshold of P<0.05 after FDR correction for multiple comparisons. Red and blue voxels represent, respectively, significant positive or inverse correlations of SRS Communication scores with rCBF values in the ASD group.

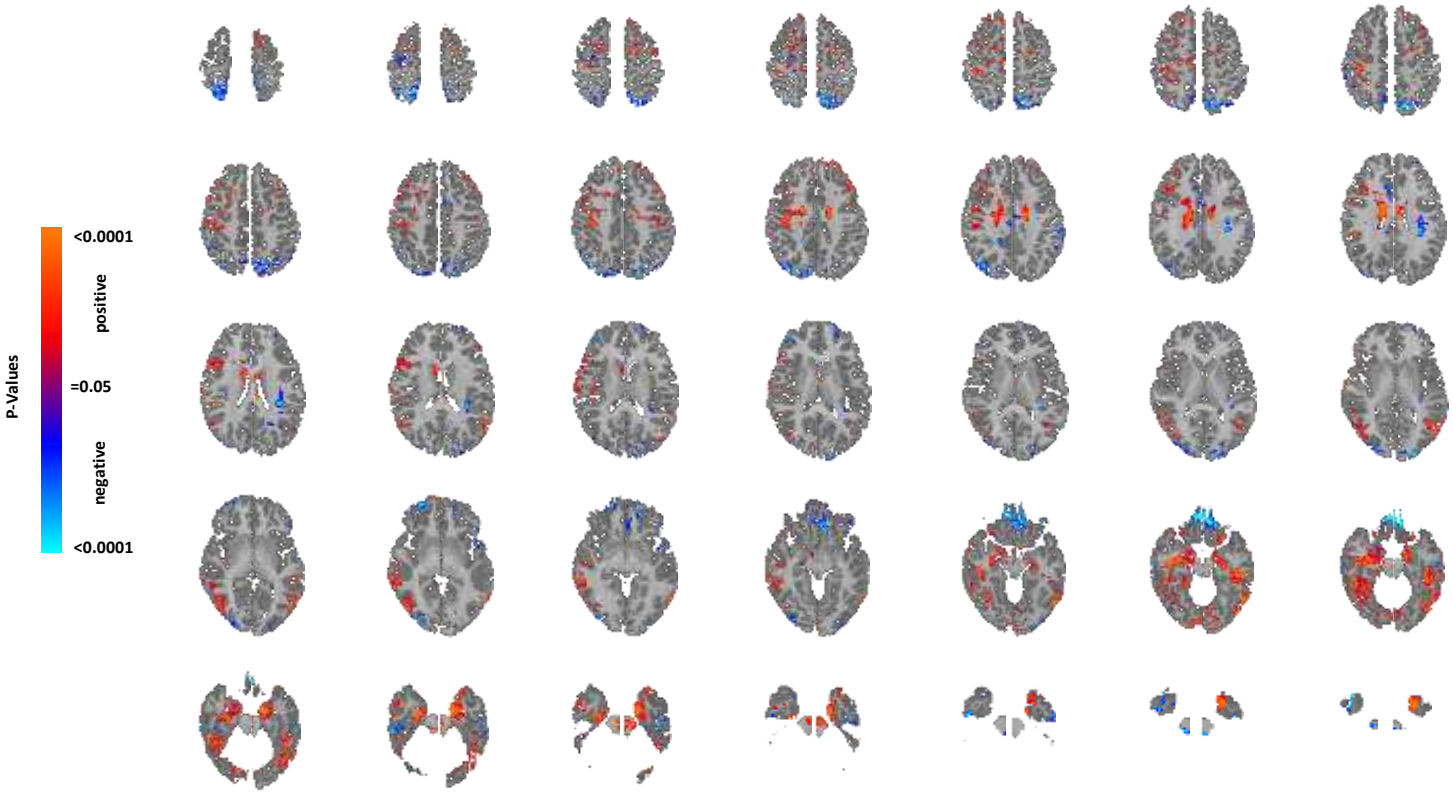

Supplementary Figure S28. Correlation of rCBF with SRS Cognition Scores for All Slices
This shows the statistically significant correlations of SRS Cognition scores with rCBF values in the ASD group for all slices while covarying for age and sex, displayed at a threshold of P<0.05 after FDR correction for multiple comparisons. Red and blue voxels represent, respectively, significant positive or inverse correlations of SRS Cognition scores with rCBF values in the ASD group.

Supplemental Materials Section 6:
Main Text Figures with Additional Covariates

Supplemental Materials Section 6a:
FSIQ Added to Base Model

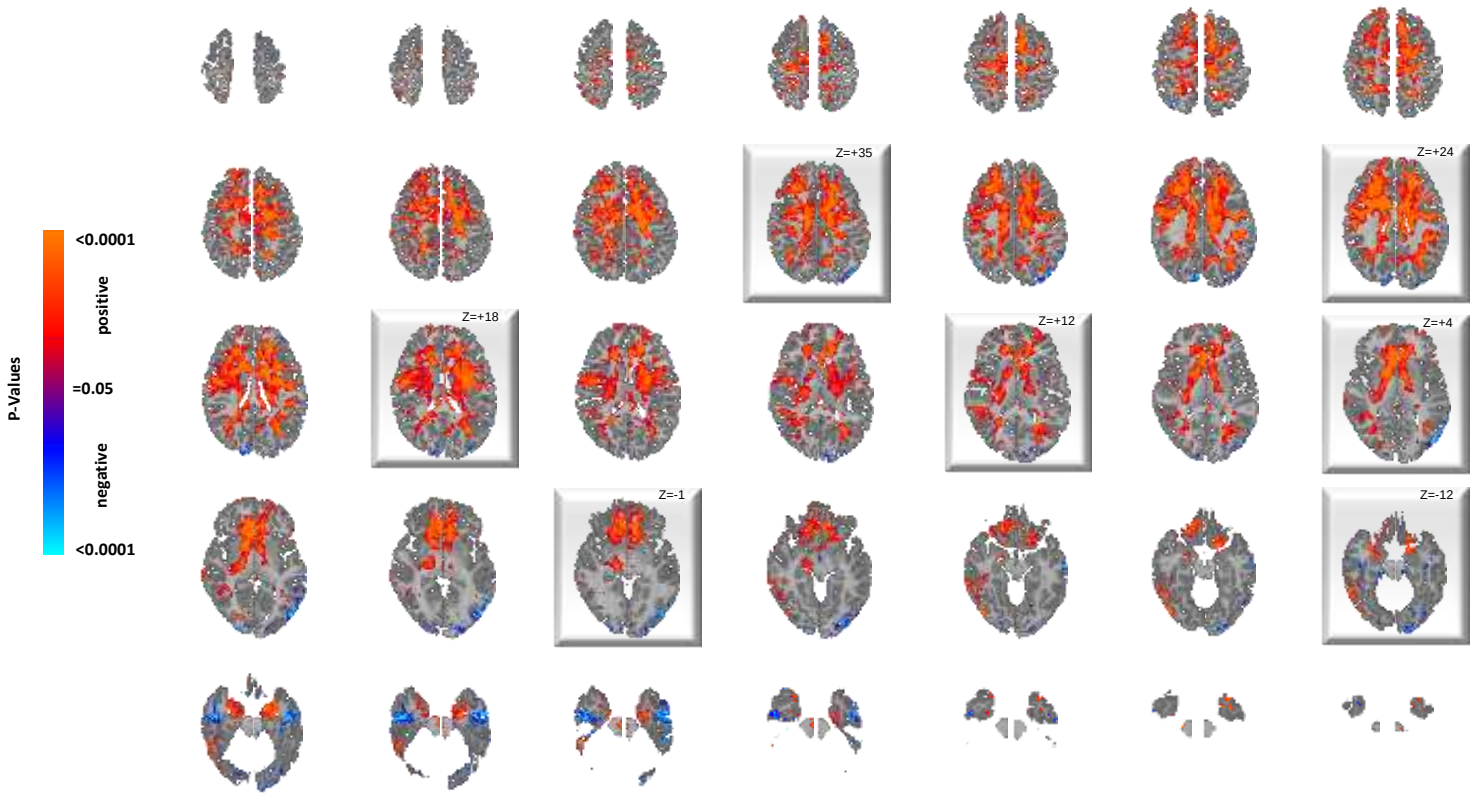

Supplementary Figure S29. Effects of Diagnosis on rCBF while Covarying for FSIQ

This shows the statistically significant differences in rCBF values between the ASD group and TD controls for all slices while covarying for age, sex, and FSIQ, displayed at a threshold of P<0.05 after correction for multiple comparisons. Voxels in red indicate significantly increased rCBF, and blue voxels reduced rCBF, in ASD relative to controls. Highlighted slices (with their z-level Talairach coordinates) are those displayed in Figure 1 of the main text.

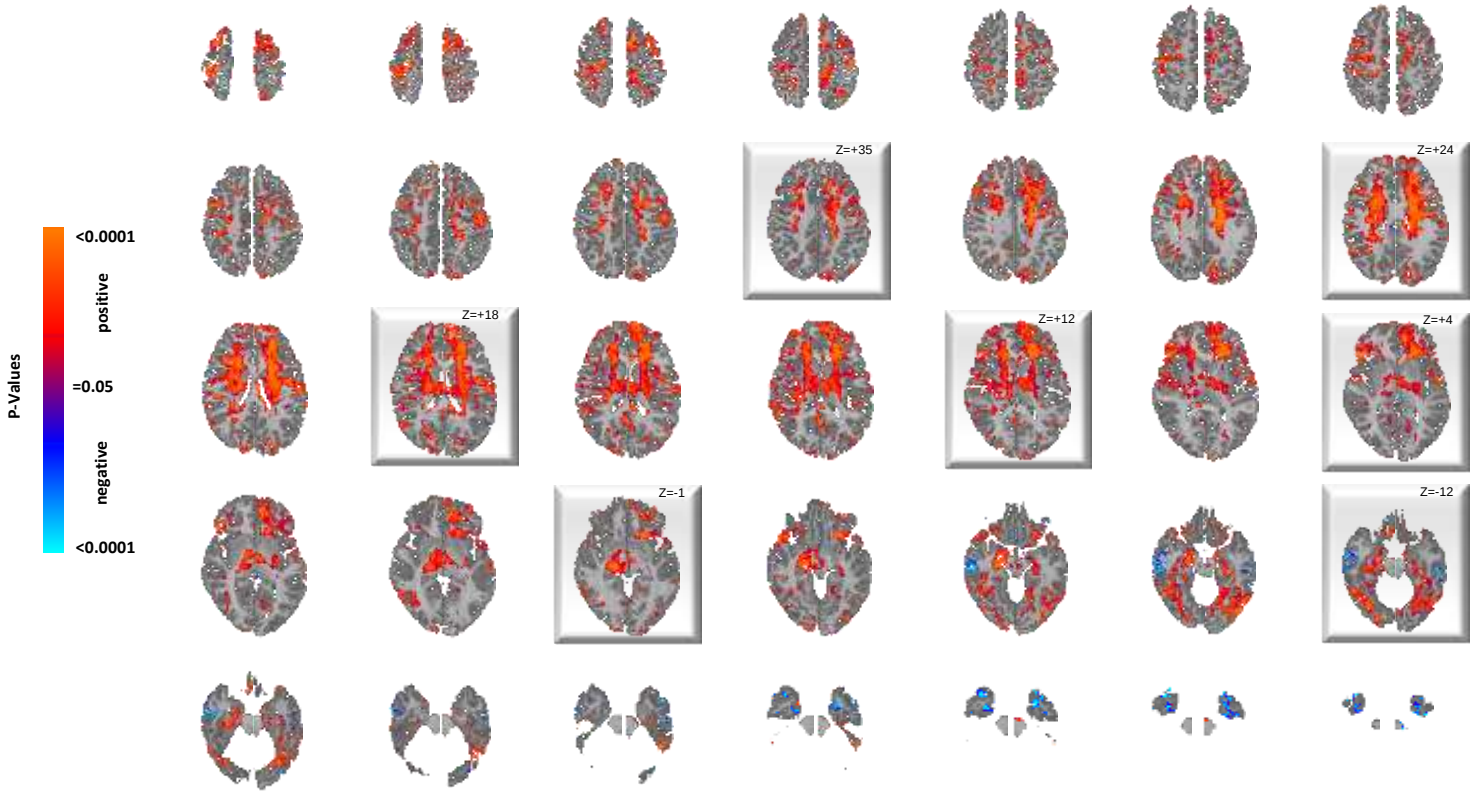

Supplementary Figure S30. Correlation of rCBF with ADOS Total Scores while Covarying for FSIQ
Shown here are all slices for the statistically significant correlations of ADOS Total scores with rCBF values in the ASD group, while covarying for age, sex, and FSIQ, displayed at a threshold of P<0.05 after FDR correction for multiple comparisons. Red and blue voxels represent, respectively, significant positive or inverse correlations of ADOS Total scores with rCBF values in the ASD group. Highlighted slices (with their z-level Talairach coordinates) are those displayed in Figure 1 of the main text.

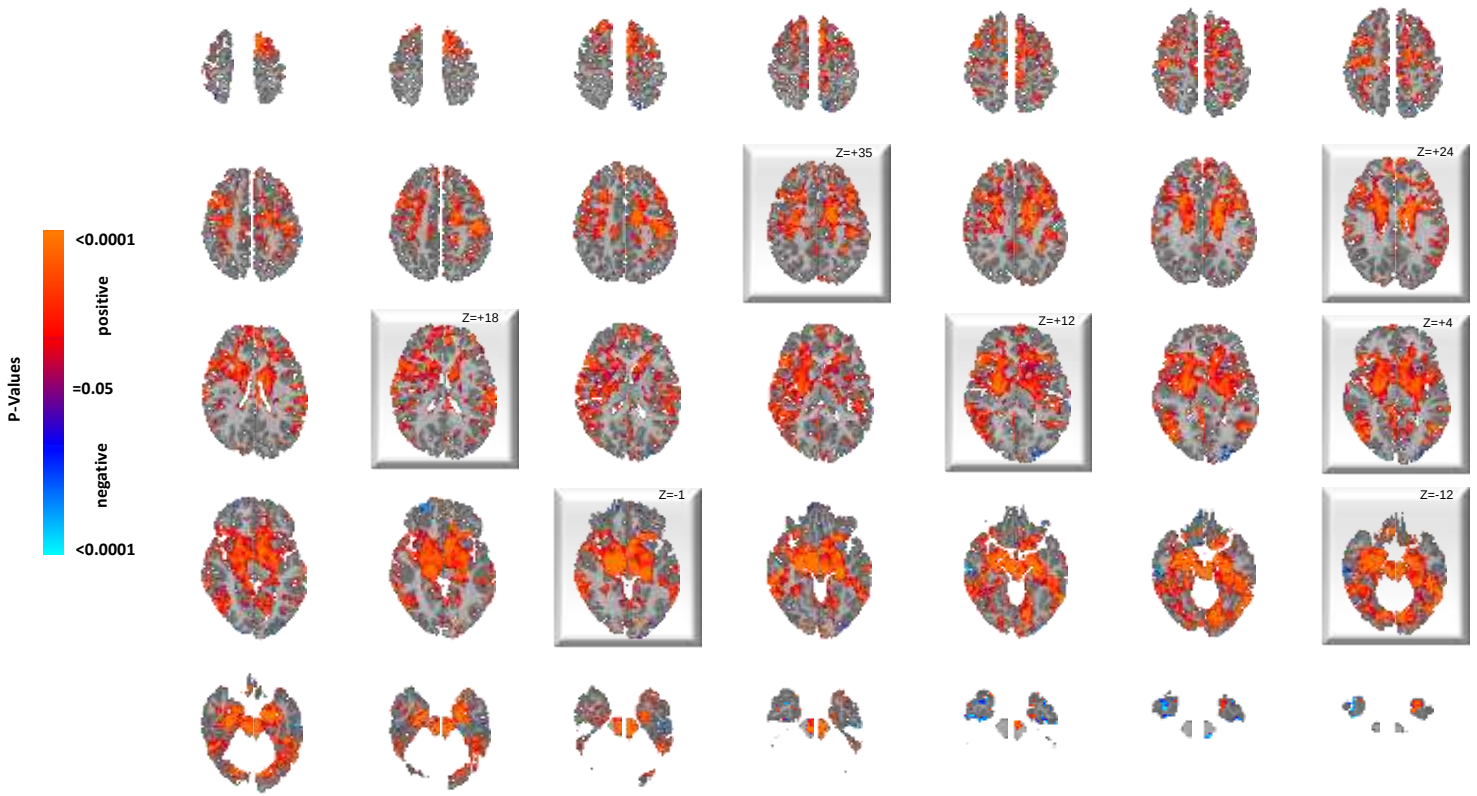

Supplementary Figure S31. Correlation of rCBF with SRS Awareness Scores while Covarying for FSIQ
Shown here are all slices for the statistically significant correlations of SRS Awareness scores with rCBF values in the ASD group, while covarying for age, sex, and FSIQ displayed at a threshold of P<0.05 after FDR correction for multiple comparisons. Red and blue voxels represent, respectively, significant positive or inverse correlations of SRS Awareness scores with rCBF values in the ASD group. Highlighted slices (with their z-level Talairach coordinates) are those displayed in Figure 1 of the main text.

Supplemental Materials Section 6b:
Psychotropic Medication Effects Added to Base Model

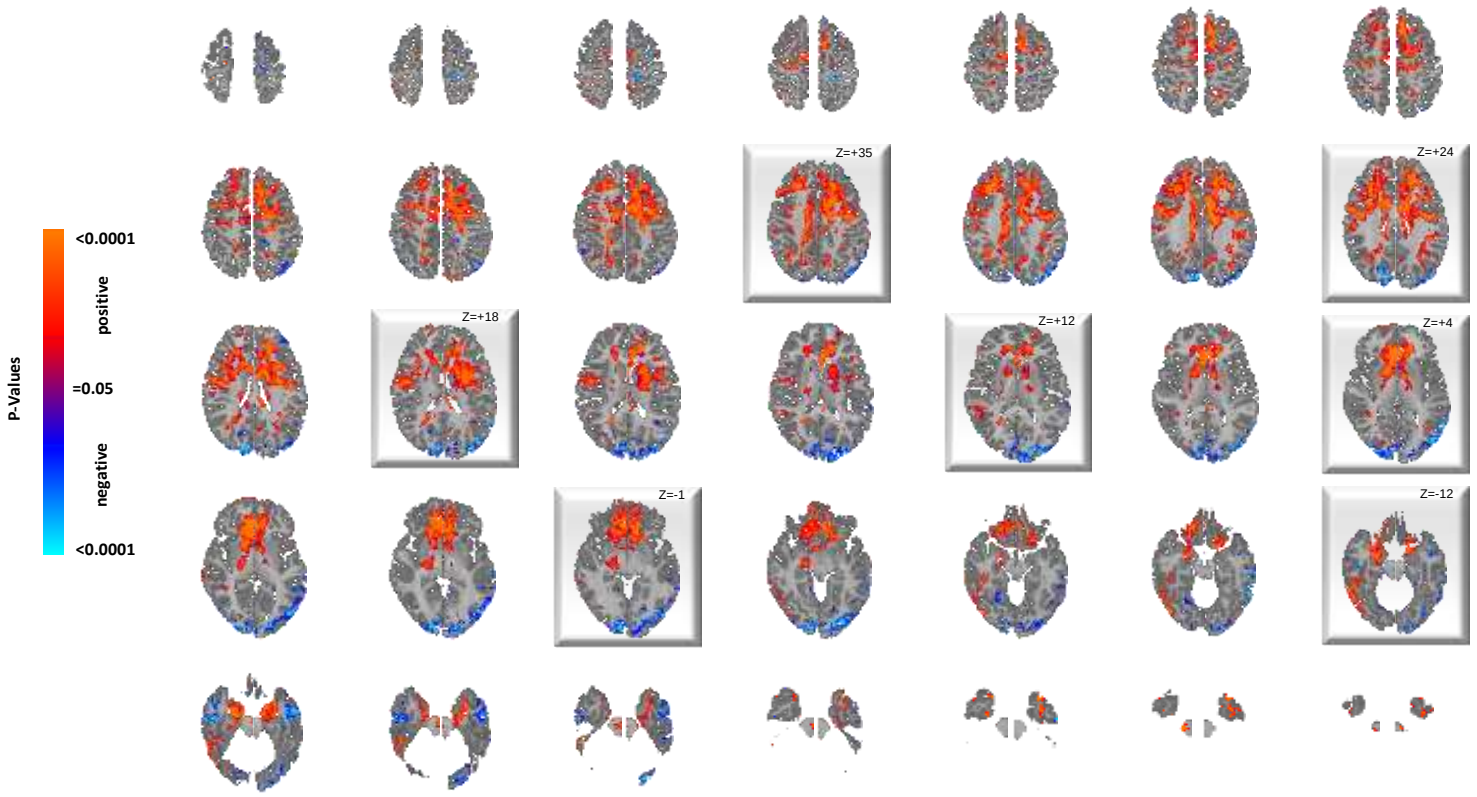

Supplementary Figure S32. Effects of Diagnosis on rCBF while Excluding ASD Participants Taking Any Psychotropic Medication
This map shows in all slices the statistically significant differences in rCBF values between a subset of the ASD group (N=29, 22 males, 7 females, mean age 23.7 years) who were not taking any psychotropic medications at the time of the MRI scan and all TD controls (N=65, 49 males, 16 females, mean age 21.6 years) while covarying for age and sex, displayed at a threshold of P<0.05 after correction for multiple comparisons. Voxels in red indicate significantly increased rCBF, and blue voxels reduced rCBF, in ASD relative to controls. Highlighted slices (with their z-level Talairach coordinates) are those displayed in Figure 1 of the main text.

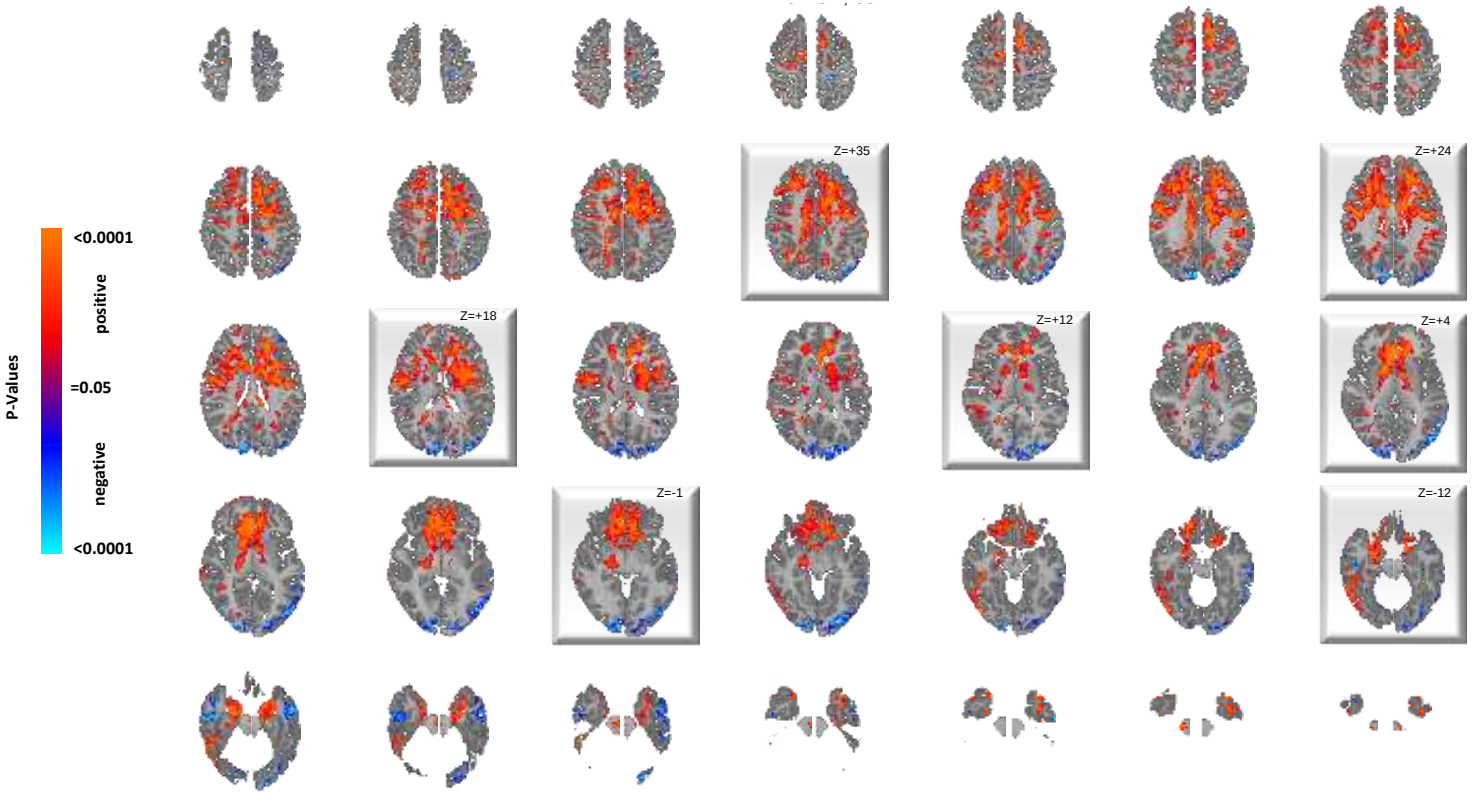

Supplementary Figure S33. Effects of Diagnosis on rCBF while Covarying for the Use of Any Psychotropic Medication at the Time of MRI Scan

This map shows in all slices the statistically significant differences in rCBF values between the ASD group (N=43, 31 males, 12 females, mean age 25.3 years) and TD controls (N=65, 49 males, 16 females, mean age 21.6 years) while covarying for age, sex, and the use of any psychotropic medication at the time of MRI scan, displayed at a threshold of P<0.05 after correction for multiple comparisons. Voxels in red indicate significantly increased rCBF, and blue voxels reduced rCBF, in ASD relative to controls. Highlighted slices (with their z-level Talairach coordinates) are those displayed in Figure 1 of the main text.

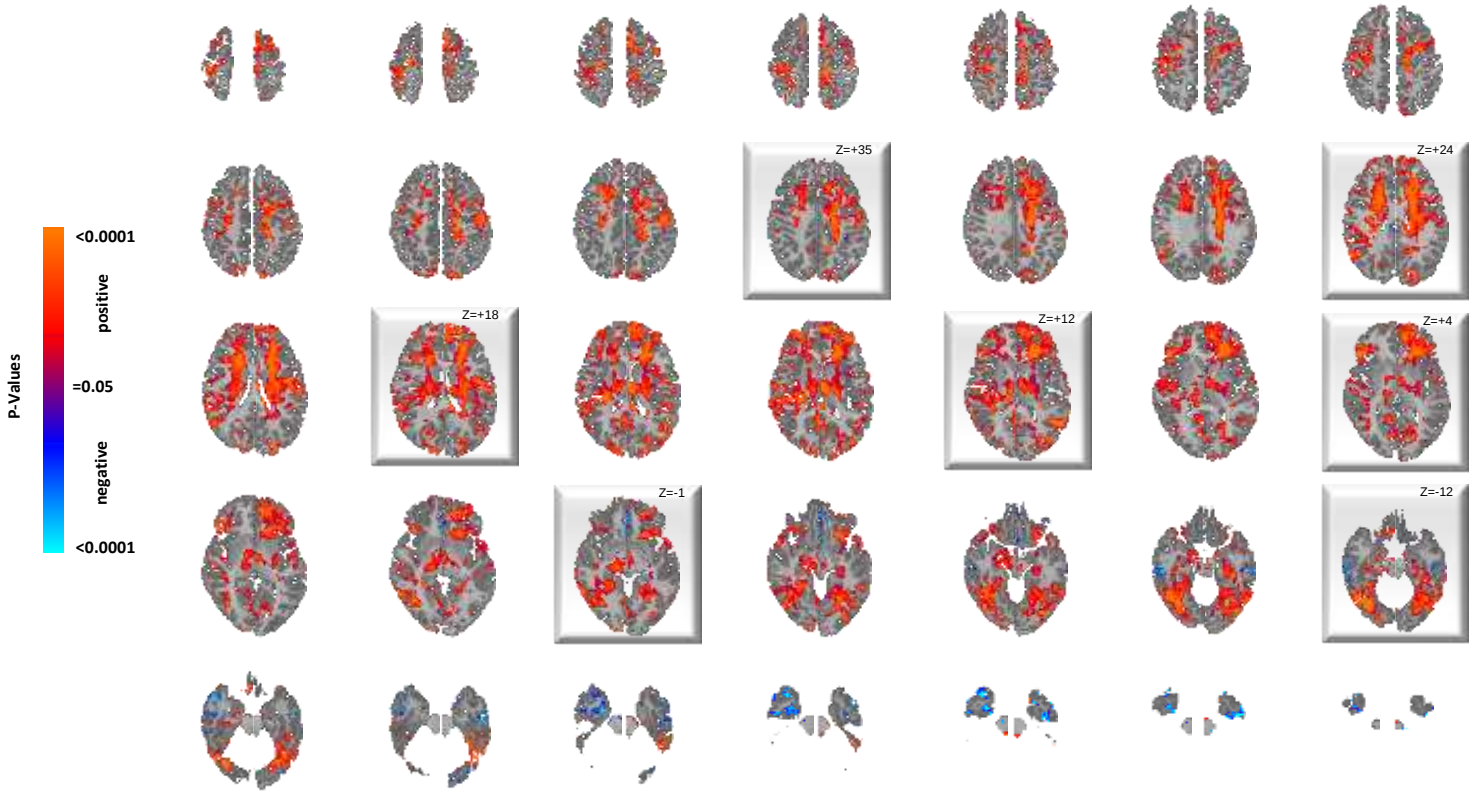

Supplementary Figure S34. Correlation of rCBF with ADOS Total Scores while Excluding ASD Participants Taking Any Psychotropic Medication
This map shows in all slices the statistically significant correlations of ADOS Total scores with rCBF values, while covarying for age and sex, in a subset of the ASD group (N=28, 21 males, 7 females, mean age 23.0 years) who were not taking any psychotropic medications at the time of the MRI scan, displayed at a threshold of P<0.05 after FDR correction for multiple comparisons. Red and blue voxels represent, respectively, significant positive or inverse correlations of ADOS Total scores with rCBF values in the ASD group. Highlighted slices (with their z-level Talairach coordinates) are those displayed in Figure 1 of the main text.

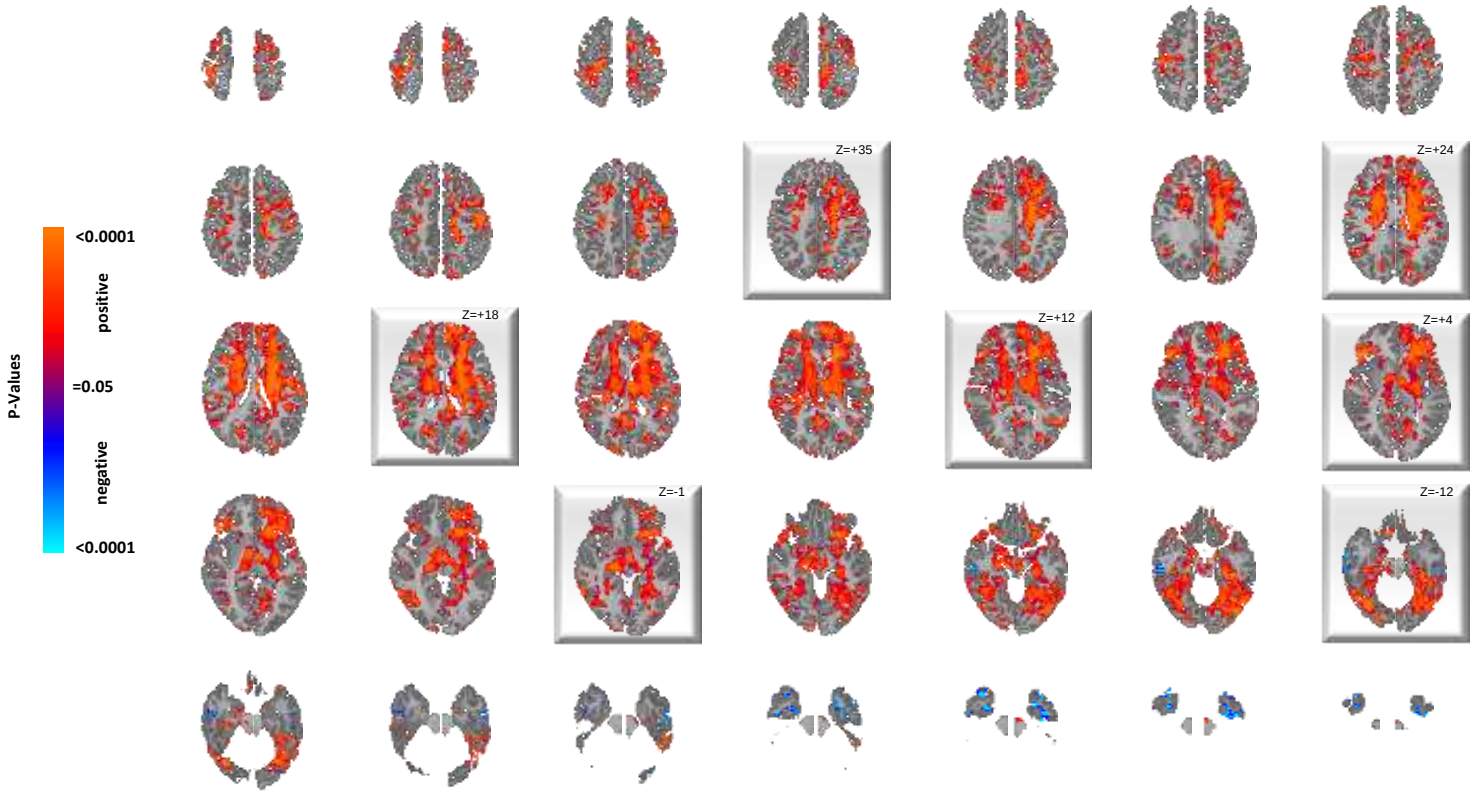

Supplementary Figure S35. Correlation of rCBF with ADOS Total Scores while Covarying for the Use of Any Psychotropic Medication
This map shows in all slices the statistically significant correlations of ADOS Total scores with rCBF values, while covarying for age and sex, for all participants in the ASD group (N=41, 30 males, 11 females, mean age 24.9 years) while covarying for age, sex, and the use of any psychotropic medication at the time of MRI scan, displayed at a threshold of P<0.05 after FDR correction for multiple comparisons. Red and blue voxels represent, respectively, significant positive or inverse correlations of ADOS Total scores with rCBF values in the ASD group. Highlighted slices (with their z-level Talairach coordinates) are those displayed in Figure 1 of the main text.

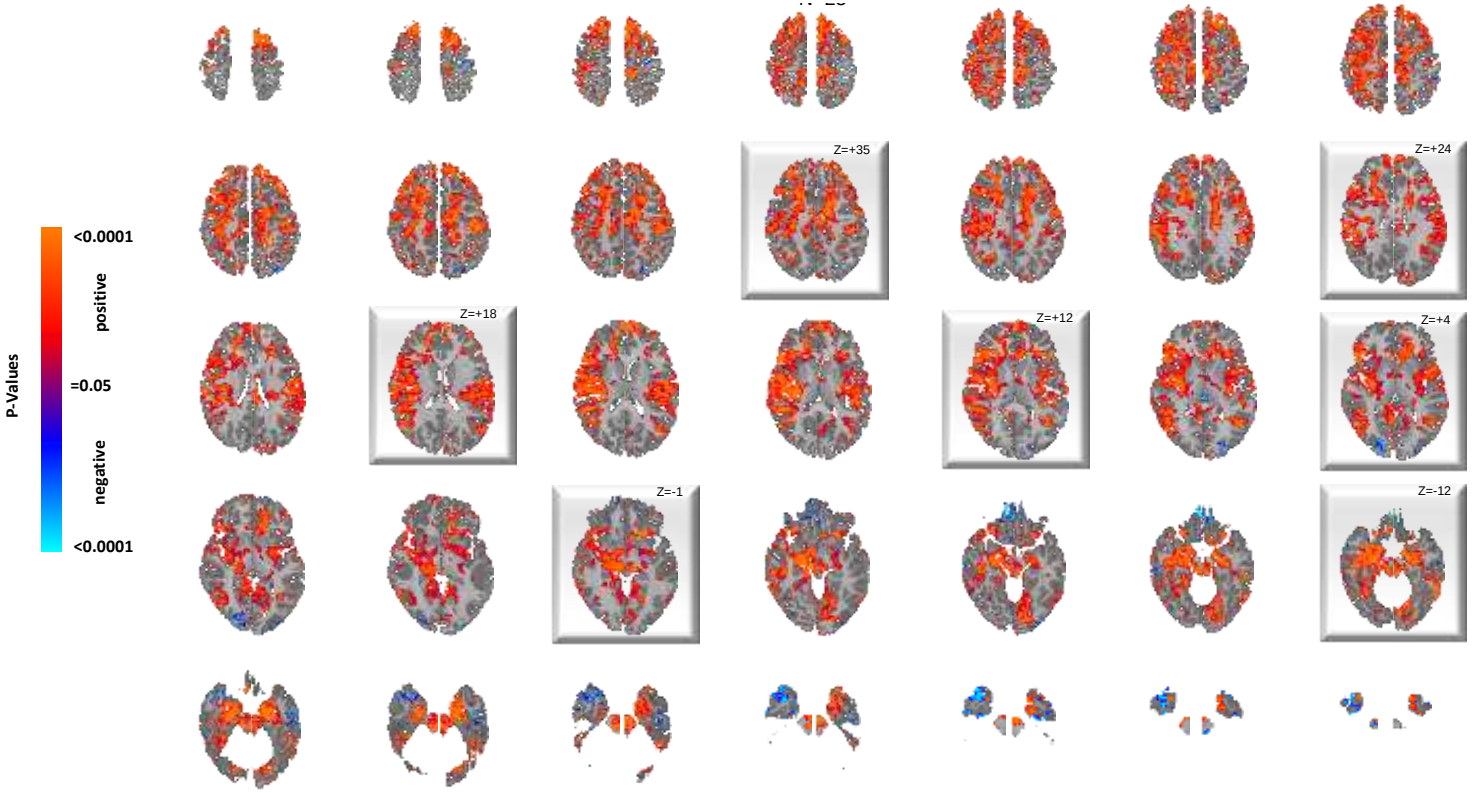

Supplementary Figure S36. Correlation of rCBF with SRS Awareness Scores while Excluding ASD Participants Taking Any Psychotropic Medication
This map shows in all slices the statistically significant correlations of SRS Awareness scores with rCBF values, while covarying for age and sex, in a subset of the ASD group (N=25, 19 males, 6 females, mean age 25.1 years) who were not taking any psychotropic medications at the time of the MRI scan, displayed at a threshold of P<0.05 after FDR correction for multiple comparisons. Red and blue voxels represent, respectively, significant positive or inverse correlations of SRS Awareness scores with rCBF values in the ASD group. Highlighted slices (with their z-level Talairach coordinates) are those displayed in Figure 1 of the main text.

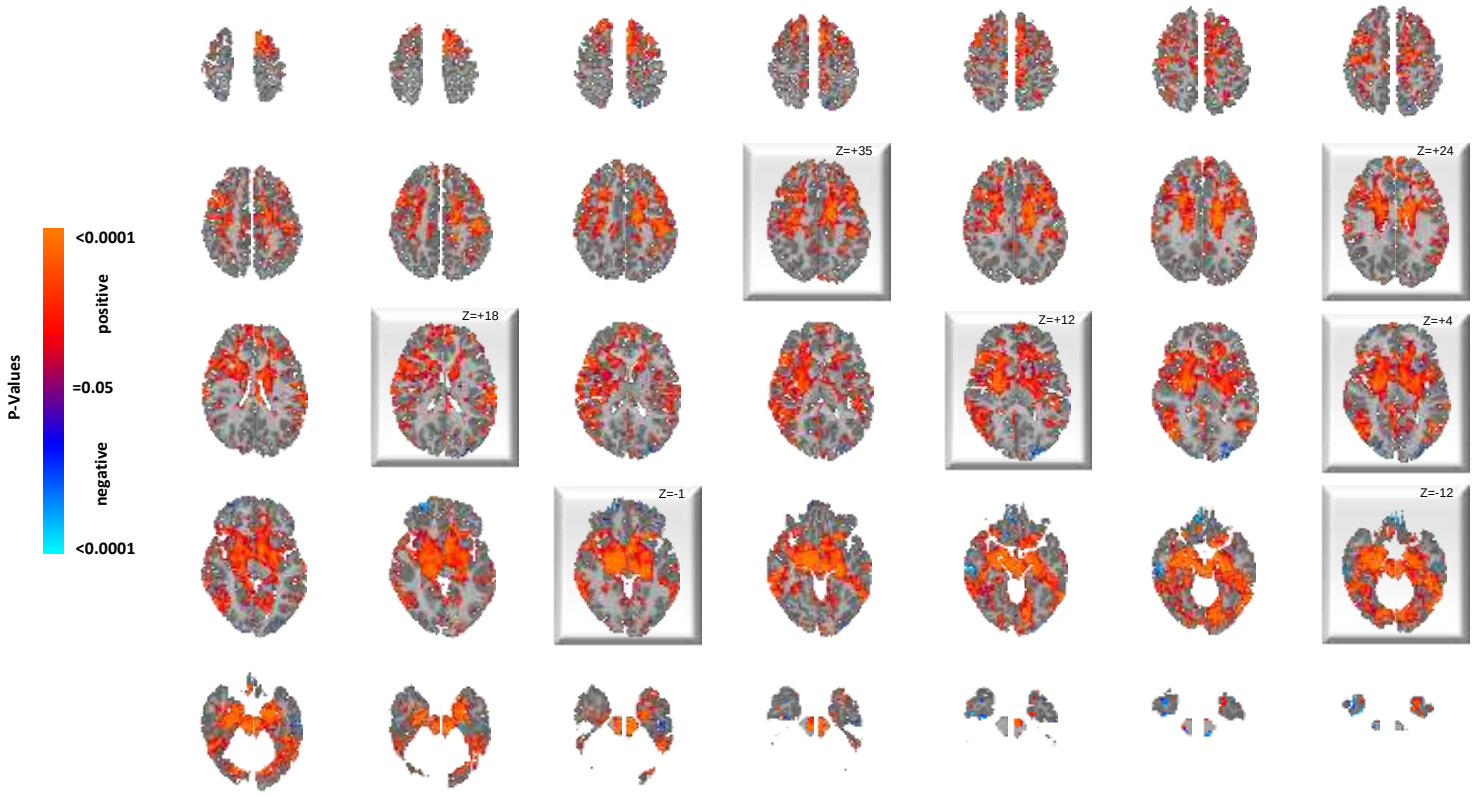

Supplementary Figure S37. Correlation of rCBF with SRS Awareness Scores while Covarying for the Use of Any Psychotropic Medication
This map shows in all slices the statistically significant correlations of SRS Awareness scores with rCBF values, while covarying for age and sex, for all participants in the ASD group (N=38, 27 males, 11 females, mean age 26.4 years) while covarying for age, sex, and the use of any psychotropic medication at the time of MRI scan, displayed at a threshold of P<0.05 after FDR correction for multiple comparisons. Red and blue voxels represent, respectively, significant positive or inverse correlations of SRS Awareness scores with rCBF values in the ASD group. Highlighted slices (with their z-level Talairach coordinates) are those displayed in Figure 1 of the main text.

Supplemental Materials Section 6c:

Total Cortical Gray and White Matter Volumes Added to Base Model

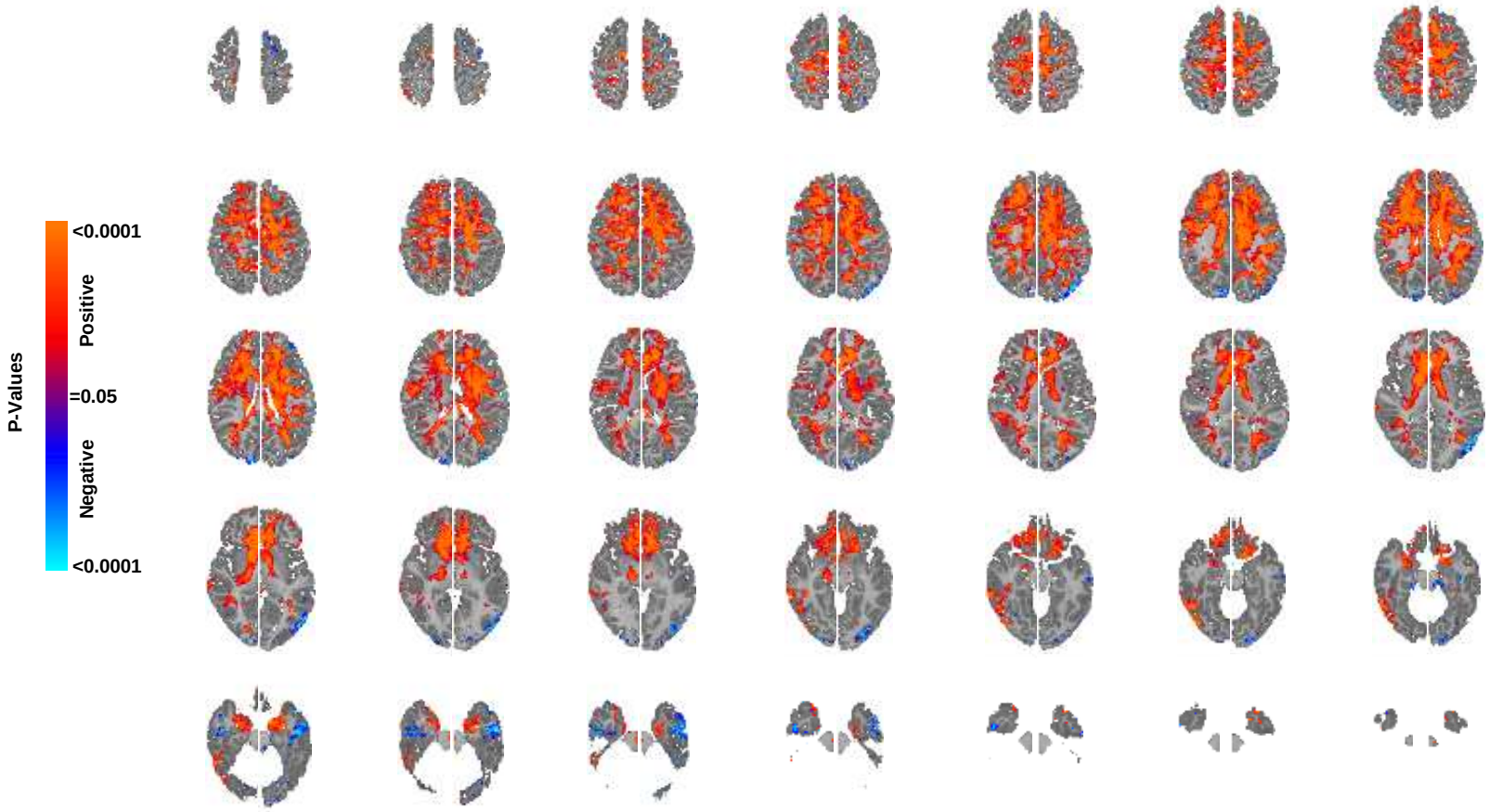

Supplementary Figure S38. Effects of Diagnosis on rCBF while Covarying for Total Cortical Gray Matter Volume
This shows the statistically significant differences in rCBF values between the ASD group and TD controls for all slices while covarying for age, sex, and total cortical gray matter volume, displayed at a threshold of P<0.05 after correction for multiple comparisons. Voxels in red indicate significantly increased rCBF, and blue voxels reduced rCBF, in ASD relative to controls.

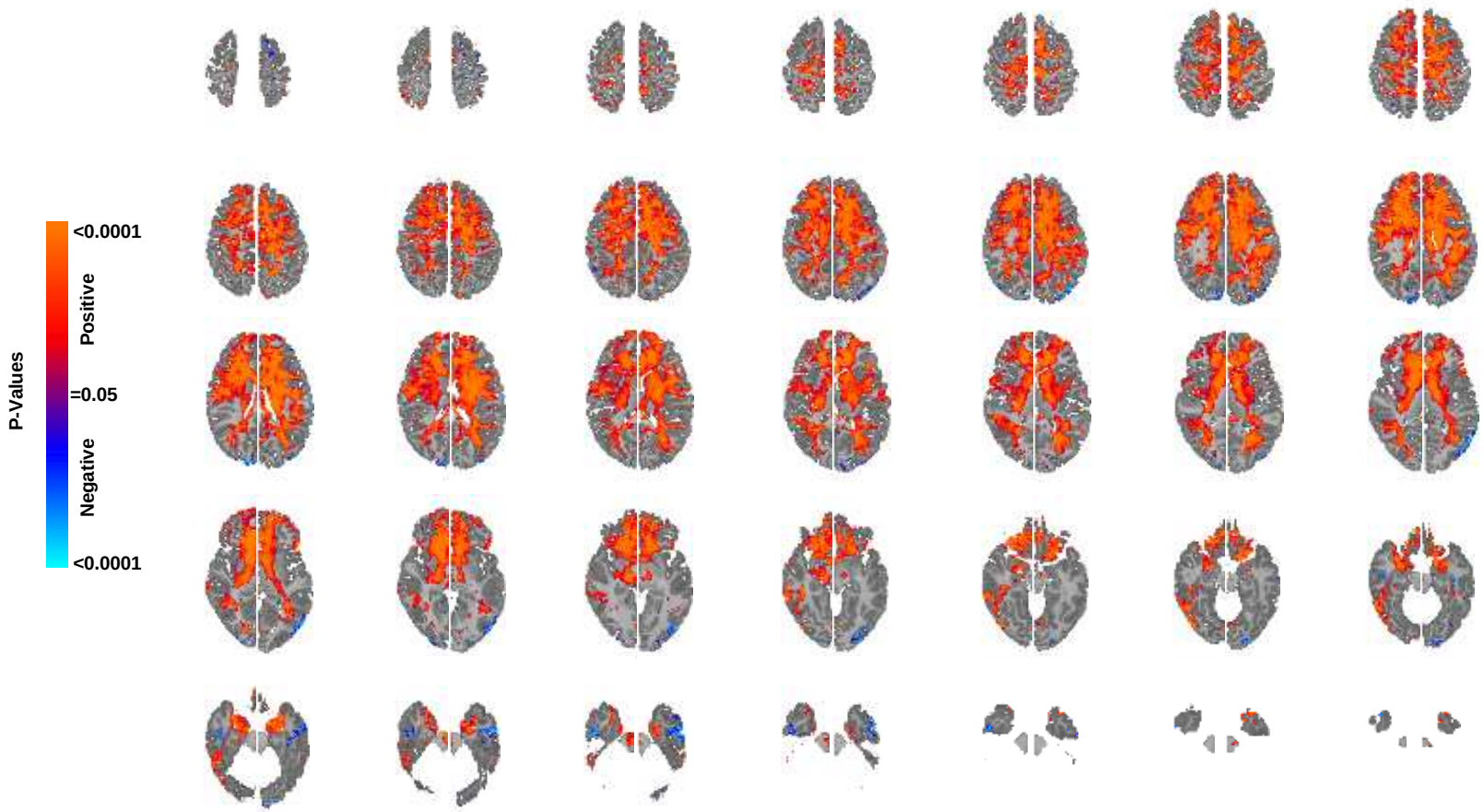

Supplementary Figure S39. Effects of Diagnosis on rCBF while Covarying for Total White Matter Volume
This shows the statistically significant differences in rCBF values between the ASD group and TD controls for all slices while covarying for age, sex, and total white matter volume, displayed at a threshold of P<0.05 after correction for multiple comparisons. Voxels in red indicate significantly increased rCBF, and blue voxels reduced rCBF, in ASD relative to controls.

Supplemental Materials Section 7:
Primary Analyses Separately in Youth and Adults

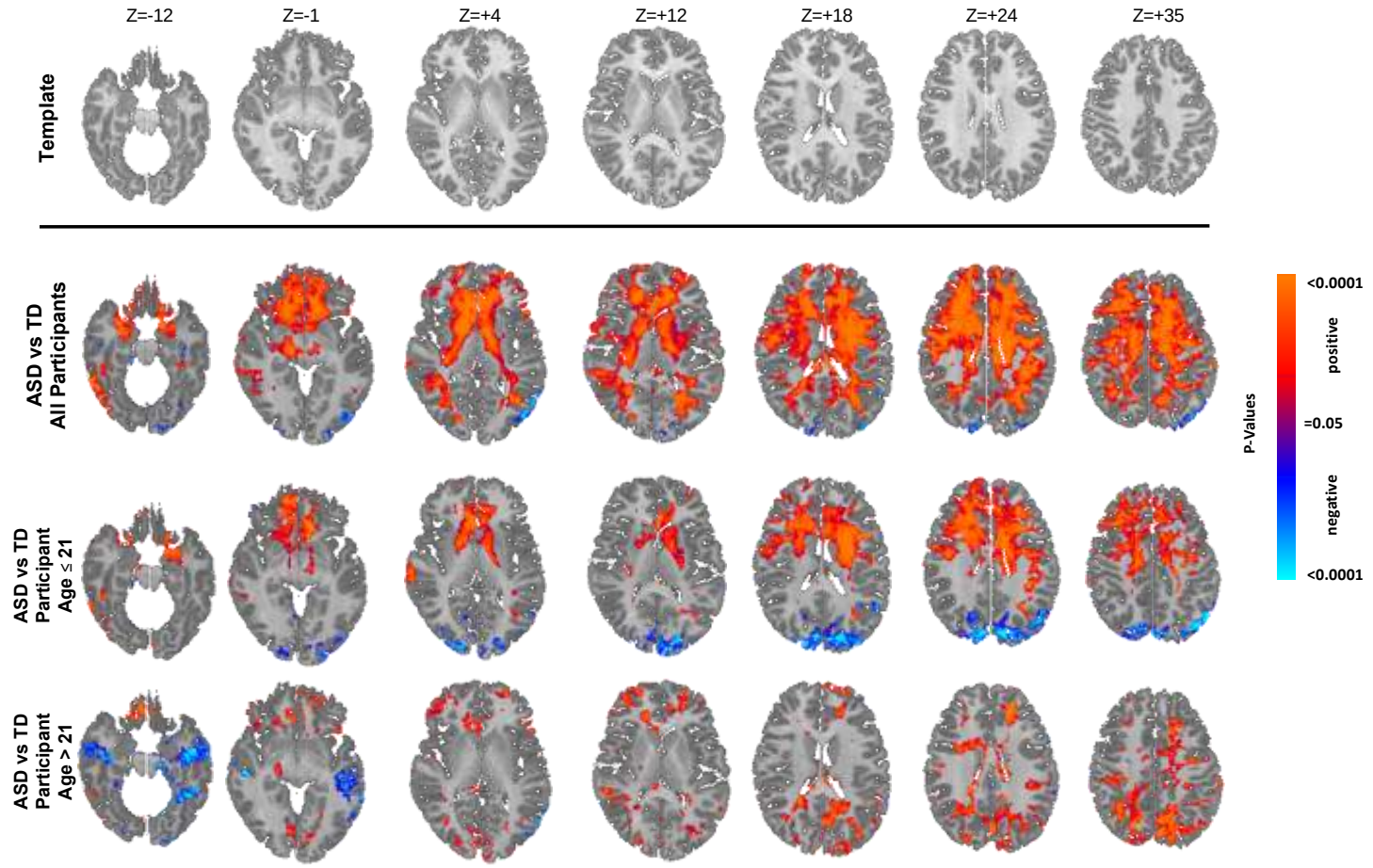

Supplementary Figure S40. Main Effect of Diagnosis Within Different Age Groups

This shows the statistically significant differences in rCBF values between the ASD group and TD controls while covarying for age and sex, separately in youth (≤21 years) and adults (>21 years), displayed at a threshold of P<0.05 after correction for multiple comparisons. Voxels in red indicate significantly increased rCBF, and blue voxels reduced rCBF, in ASD relative to controls.

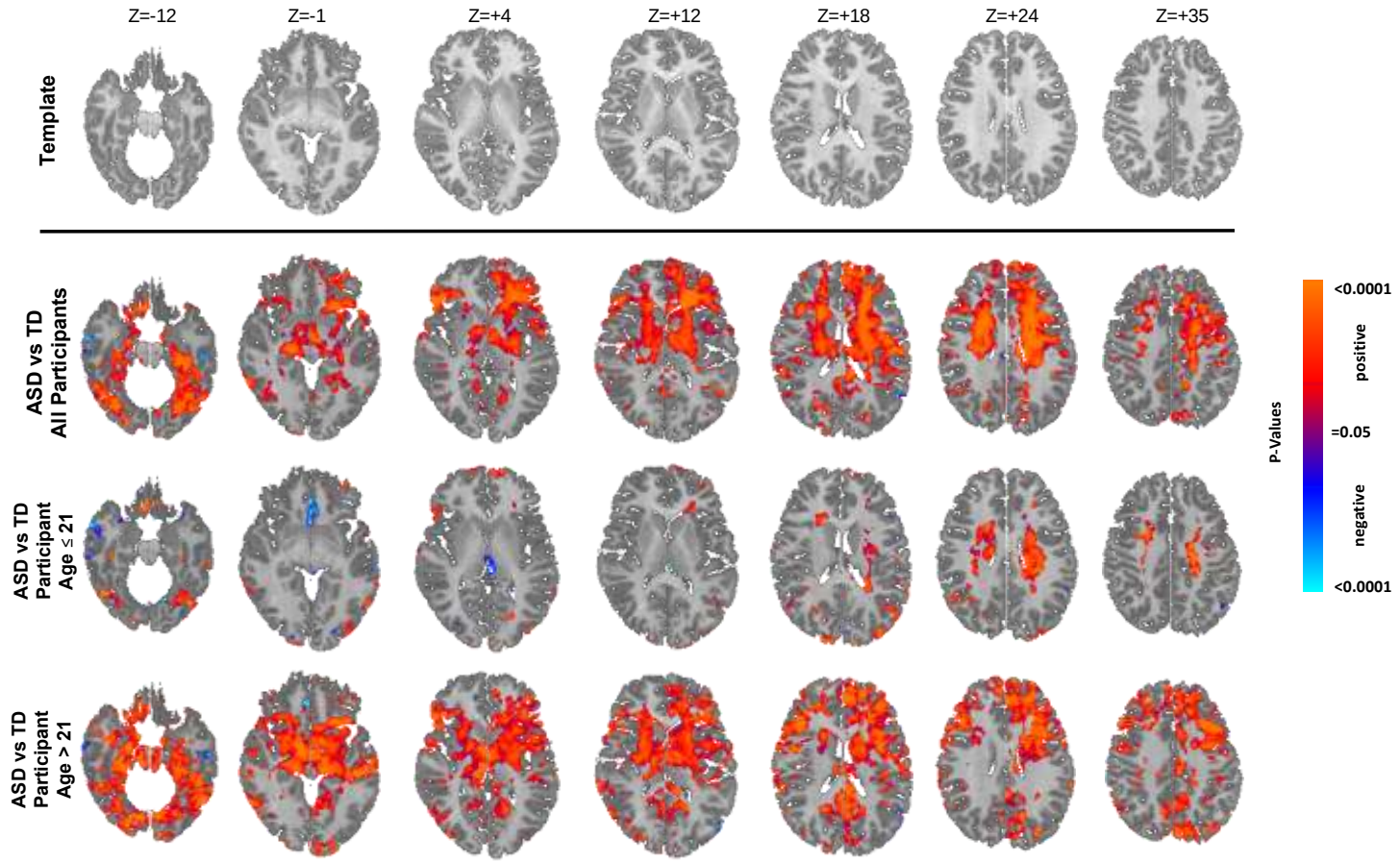

Supplementary Figure S41. Correlation of rCBF with ADOS Total Scores Within Different Age Groups

Red and blue voxels represent, respectively, significant positive or inverse correlations of ADOS total scores with rCBF values separately in youth (≤ 21 years) and adults (>21 years) of the ASD group, after FDR correction for multiple comparisons.

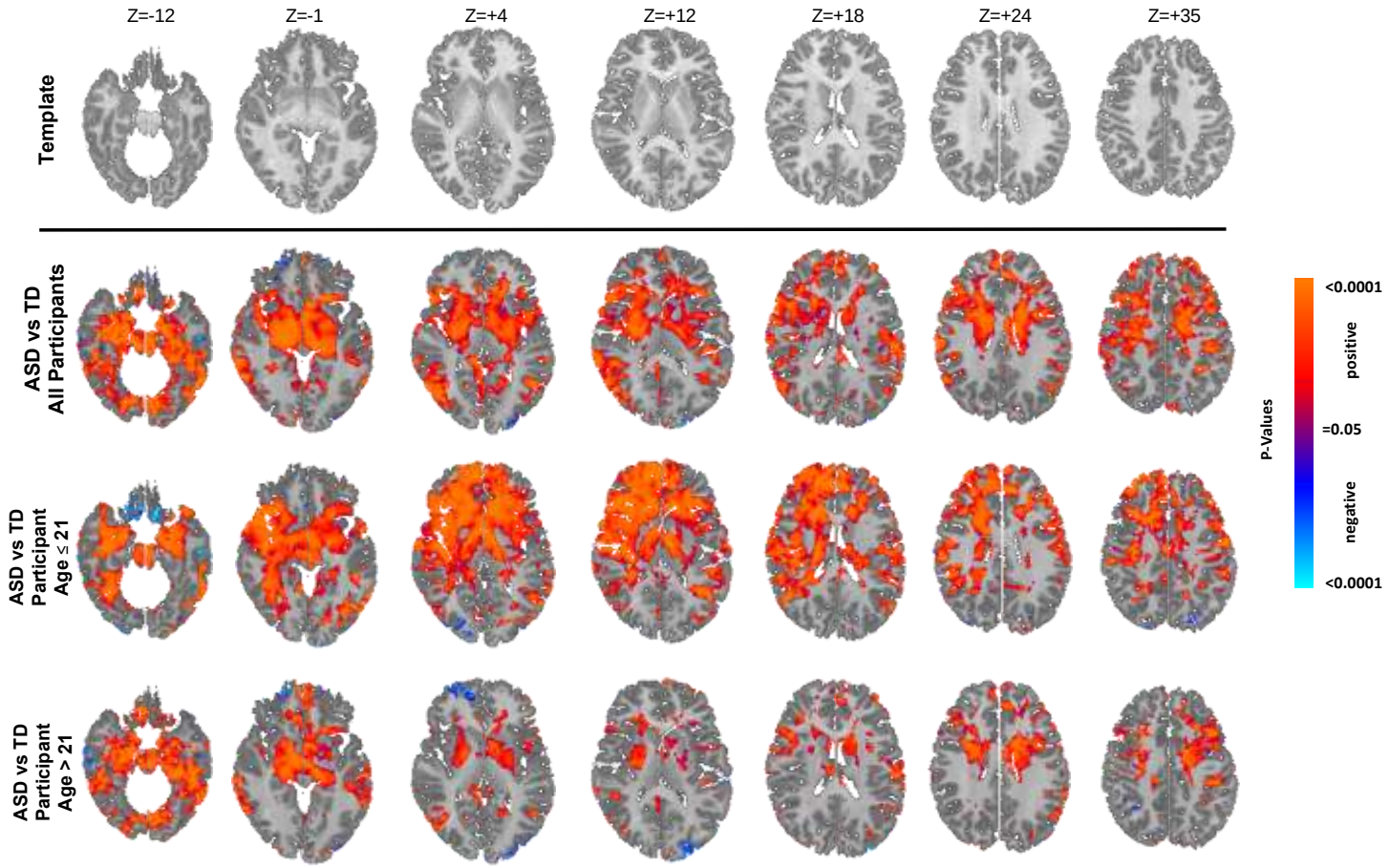

Supplementary Figure S42. Correlation of rCBF with SRS Awareness Scores Within Different Age Groups
Red and blue voxels represent, respectively, significant positive or inverse correlations of SRS Awareness scores with rCBF values separately in youth (≤ 21 years) and adults (>21 years) of the ASD group, after FDR correction for multiple comparisons.